https://doi.org/10.5194/egusphere-2025-6216
Preprint. Discussion started: 20 January 2026

Km-scale regional coupled system for the Northwest European shelf for weather and climate applications: RCS-UKC4

Ségolène Berthou[1], Juan Manuel Castillo[1], Vivian Fraser-Leonhardt[2], Sana Mahmood[1], Nefeli Makrygianni[1], Alex Arnold[1], Claudio Sanchez[1], Huw Lewis[1], Dale Partridge[3], Martin Best[1], Lucy Bricheno[4], Helen Davies[5], Douglas Clark[5], James R. Clark[3], Jeff A. Polton[4], Andrew Saulter[1], Chris J. Short[6], Jonathan Tinker[1], Simon Tucker[6]

[1] Met Office, Exeter, United Kingdom
[2] University of Reading, Reading, United Kingdom
[3] Plymouth Marine Laboratory, Plymouth, United Kingdom
[4] National Oceanography Centre, Liverpool, United Kingdom
[5] UK Centre for Ecology and Hydrology, Wallingford, United Kingdom
[6] Met Office Hadley Centre, Exeter, United Kingdom

Correspondence to: segolene.berthou@metoffice.gov.uk

Abstract. Increasing the complexity of regional weather and climate models by developing coupled environmental prediction systems increases prediction skills in coastal areas, where equilibrium assumptions between Earth system components break down. By allowing consistency between earth system components, they also unlock new insights on multi-hazard processes with benefits for enhanced forecasting. We present recent advances in the regional coupled environmental prediction system developed in the UK through the release of the Regional Coupled Suite – UK Coupled domain version 4 (RCS-UKC4) configuration. This includes implementation of the new Regional Atmosphere and Land configuration (RAL3.3) alongside updates to all model components relative to previous releases. RCS-UKC4 also supports enhanced online simulation of river flows and coupling to a biogeochemistry model. New functionality including running near-real time ensemble forecasts and climate hindcasts is demonstrated. We first examine the effects of changing atmospheric and land configurations in both multi-annual simulations and short-term forecasts and assess the quality of river flows. RAL3.3 shows a beneficial increase in shortwave radiation reaching the ocean in summer months and a beneficial reduction in wind speed, which is slightly further reduced with wave coupling. River discharges have good skill in the northern and western regions of the UK, whilst the southeast rivers show too much variability. In a second part, we introduce ensemble forecasts, and show RCS-UKC4 has good skill in terms of wave forecasts during storms compared to the current operational ensemble: it shows lower root mean square error thanks to a good representation of tidal current/wave/wind interactions. Coupling can either increase or decrease the ensemble spread in screen temperature relative to atmosphere-only ensemble simulations, depending on whether latent heat flux or radiative heat flux dominates the spread in near-surface fluxes. Finally, we demonstrate that higher frequency (10-minute coupling) enables new prediction capability with a good representation of high frequency sea surface height variability linked with weather disturbances.

https://doi.org/10.5194/egusphere-2025-6216
Preprint. Discussion started: 20 January 2026

1 Introduction

Coastal regions are complex environments providing weather forecasting challenges due to the strong influence of both land and sea (Holt *et al.*, 2017; Cavaleri *et al.*, 2018). On longer time-scales, regional climate change is strongly modulated by a differential warming rate between land and sea (Kendon *et al.*, 2010). Regional coupled systems are therefore increasingly being used for both weather forecasting (Durnford *et al.*, 2018; Komaromi *et al.*, 2021) and climate projections (Ruti *et al.*, 2016; Somot *et al.*, 2018), though their technical complexity and administrative separation of marine and land forecasts and projections restrict their widespread use (Berthou et al., 2025a).

Nevertheless, Berthou et al. (2025a) highlight the many benefits of forecasts and projections enabled by consistent treatment of heat and momentum exchange in coupled systems. The United Kingdom is located on the Northwest European shelf (NWS), which is a shallow continental shelf sea region (<250m) where tidal energy is dissipated through strong tidal currents surrounding the British Isles. Deeper regions of the NWS become stratified in summer (e.g. North Sea), while shallower regions remain mixed throughout the column (e.g. Channel, Irish Sea). These strong tidal currents modulate wave height (Cavaleri *et al.*, 2018) and even wind speed, which makes this region one of the few mid-latitude regions where the ocean dissipates tidal energy by modulating atmospheric wind (Renault & Marchesiello, 2022). In the mid-latitudes, the ocean feedback on the atmosphere remains weak, as pressure gradients are set by atmospheric baroclinicity, not by sea surface temperature (SST) gradients, and because deep convection is not a dominant driver of atmospheric variability. Nevertheless, it is now widely known that the ocean modulates the atmosphere at small time and space scales, such as over eddies, strong SST gradients and western boundary currents (Sheldon *et al.*, 2017; Vannière *et al.*, 2017). As weather and marine forecasting now reach better accuracy at kilometric scale, these interactions become non-negligible.

The Met Office currently operates a regional km-scale coupled wave/ocean deterministic forecast driven by its global coupled model (Guiavarc'h *et al.*, 2019). This waves/ocean system shows benefits for predicting sea surface temperature, surface currents during storms and extreme waves and surge (Lewis *et al.*, 2019b; Bruciaferri *et al.*, 2021). Since May 2022, this system now sends its SST forecast to the regional atmospheric forecast. This change improved weather forecasts of air temperature during early summer and late autumn, when 5-day SST evolution is non-negligible (Mahmood *et al.*, 2021), in particular during marine heatwaves (Berthou et al., 2024). Around fifty percent of the improvements brought by the May 2022 regional operational suite upgrade came from changing the SST from a fixed observed value to a deterministic ocean forecast (Met Office personal communication); the added value is clear even in 36h forecasts in marine heatwave onset conditions (Berthou et al., 2024). In addition, sending hourly SST to the atmosphere also provided improvements to coastal fog forecasting when the SST diurnal cycle plays a role in fog formation (Fallmann *et al.*, 2019).

These improvements to the operational system were enabled by Met Office investment in the development of a flexible research framework for km-scale regional coupling (Lewis *et al.*, 2018, 2019a). Based on this system, (Gentile *et al.*, 2021, 2022) and (Valiente *et al.*, 2021) explored the benefits of coupling a wave model with the atmosphere and highlighted that a consistent treatment of momentum transfer between the atmosphere and the ocean is crucial for wave and wind forecasting, in

https://doi.org/10.5194/egusphere-2025-6216
Preprint. Discussion started: 20 January 2026

particular during storms. Indeed, wind speed around the complex coastline of the British Isles is particularly difficult to forecast because of the intricate combination of land/sea roughness contrast, non-stationary ocean surface (strong tidal currents), breaking or growing waves and complex wave reflection at the coast.

In this article, we present a new version of the Regional Coupled Suite – UK Coupled domain version four (RCS-UKC4), which brings corrections and enhancements to the UKC3 system (Lewis et al., 2019a). We document a) the impact of upgrading the atmosphere and land configuration on the coupled system, in particular its SST, winds and river discharge; b) introduce the ensemble forecasting capability, to show a regional coupled system offers promises for improved ensemble wave and wind forecasting, show sensitivity tests for further wind/wave improvements and explain how a coupled ensemble modulates the ensemble spread of air temperature; c) we show how increased 10mn coupling enables the representation of meteotsunamis, which current operational systems can't currently forecast. RCS-UKC4 also includes an option to couple a biogeochemistry model in the ocean to represent the ocean colour, chemistry and lower trophic levels of biology (phyto- and zooplankton). The addition of a biogeochemistry system is further documented in a companion paper (Partridge *et al.*, 2025).

2 Description of the coupled system

2.1 Updates in RCS-UKC4 from UKC3

Since UKC3 (Lewis *et al.*, 2019a), the Regional Coupled Suite has been developed as a modular framework for fully or partially coupled configurations and supports two main domains: one centred over India: RCS-IND1 (Castillo et al., 2022) and one over the United Kingdom: RCS-UKC4. UKC3 was only supporting deterministic case studies (5-day forecasts), whereas ensemble (past or near-real time) forecasts (Gentile *et al.*, 2022) and climate hindcasts are now supported in RCS-UKC4. We present the RCS-UKC4 configuration, coupling the Unified Model (UM) (Cullen, 1993; Brown *et al.*, 2012), the Joint United Kingdom Land Environment Simulator (JULES) (Best et al., 2011), the Nucleus for European Modelling of the Ocean (NEMO) (Madec *et al.*, 1998), WAVEWATCH III (Tolman & the WWIII development group, 2014) and the European Regional Seas Ecosystem Model (ERSEM) (Butenschön *et al.*, 2016) over a domain covering the Northwest European shelf (Fig. 1). The UM has a variable resolution from 4.4km to either 1.5km in deterministic forecasts (UKV) or 2.2km in ensemble forecasts or climate runs (ENUK), on a rotated pole. NEMO and ERSEM share the same rotated pole at the atmosphere, but on a regular ~1.5km fixed resolution (Graham *et al.*, 2018). WAVEWATCH III uses a Spherical Multi-Cell grid with 3km in the open ocean down to 1.5km at the coast (Li, 2022), also using the same rotated pole grid. The UM and JULES are coupled at the timestep level with the method described in (Best *et al.*, 2004). The UM, NEMO and WAVEWATCHIII exchange fields through the Ocean Atmosphere Sea Ice Soil 3 - Model Coupling Toolkit (OASIS3-MCT) coupling library (Valcke, 2013), which handles the regridding and timing of field exchanges. NEMO and ERSEM are coupled with the Framework for Aquatic Biogeochemical Models (FABM) coupler (Bruggeman & Bolding, 2014), which handles 3D fields on the same grid. The additional biogeochemisty capability of the coupled system is documented in a companion paper (Partridge et al., 2025).

https://doi.org/10.5194/egusphere-2025-6216
Preprint. Discussion started: 20 January 2026

Compared to UKC3, the models have been upgraded to the state-of-the-art model versions:

- UM v13.5, with options of running three Regional Atmosphere and Land configurations: RAL1 (Bush *et al.*, 2020), RAL2 (Bush *et al.*, 2023) or the newest RAL3.3 (Bush *et al.*, 2024), requiring additional branches in UM v13.5[1]. Note that in this paper, RAL3.2 is also sometimes used, as at the times of the trials, it was the latest version. The main difference between RAL3.2 and RAL3.3 relevant to this paper is an increase in low-level cloud cover in anticyclonic conditions from changes in monotonicity scheme for moisture advection, and further changes to make the radiation scheme more consistent with the use of CASIM microphysics (Bush *et al.*, 2024).
- JULES v7.5, with an additional JULES branch[1] to run online river routing with the River Flow Model (RFM). Online RFM was implemented and documented by (Lewis & Dadson, 2021).
- NEMOv4.0.4 for the Atlantic Margin Model 1.5km (AMM15) domain (Patmore *et al.*, 2023)
- WAVEWATCH III v7.12 (Tolman & the WWIII development group, 2014)
- ERSEM v15.06 (Butenschön *et al.*, 2016)

In a coupled system, changes in one component will inevitably affect the others: this article documents the journey undertaken from changing individual model versions and configurations to having a final coupled configuration. Table 1 shows the main differences in UKC4 compared to UKC3, focusing on changes to the model science configuration most relevant to this work: the full set of changes is documented in Table 1 and 2 of (Bush *et al.*, 2024). The coupling terms have changed since UKC3, but have been documented for the India domain in (Castillo et al., 2022), the only term which was changed since then was exchanging 10m neutral winds instead of actual 10m winds, documented in section 3.2. The coupling frequency has been increased from 1h to 10mn, documented in section 4, light penetration value has been reverted to the same value as the current operational wave/ocean coupled system (Tonani et al., 2019), highlighted in section 3.1.

[1] The UM and/or JULES code used in the publication has been committed to the UM and JULES code trunks, having passed both science and code reviews according to the UM and JULES working practices. Please note, at the time of the work for this paper they were branches to UM/JULES versions stated in the paper.

https://doi.org/10.5194/egusphere-2025-6216
Preprint. Discussion started: 20 January 2026

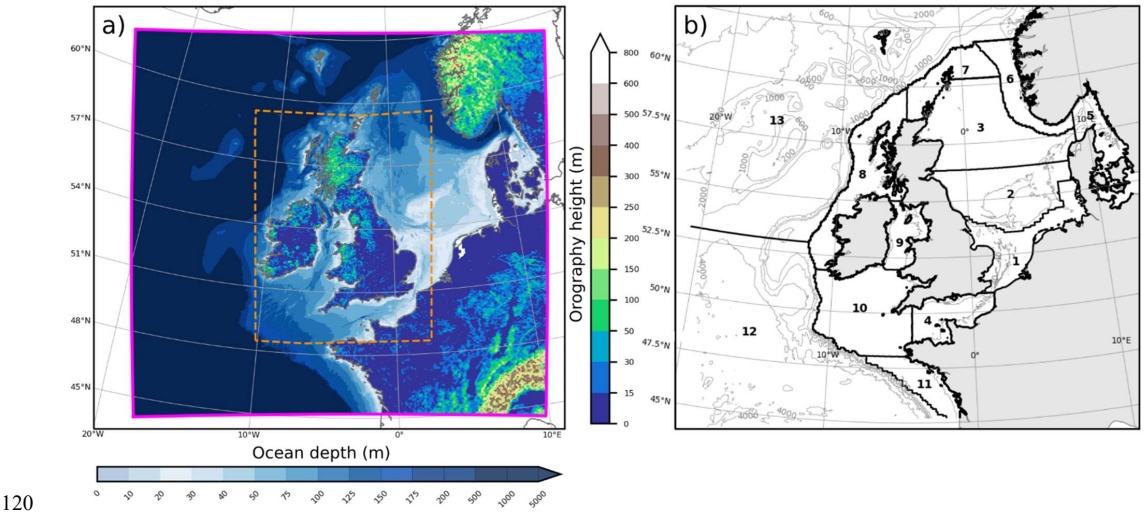

Figure 1: a) UKC4 domain extent (same as UKC3), ocean bathymetry and orography. Orange dotted line shows the atmospheric inner domain with 2.2km resolution, outside this domain, the atmosphere runs on a 4.4km/4.4km grid in the corners, and mixed 4.4/2.2km in the outer middle sections. The ocean has a regular 1.5km grid, the waves have variable 3km-1.5km resolution, 1.5km close to the coast. b) hydrodynamic regions of the domain as defined by (Wakelin *et al.*, 2012), regions 1-11 delineate the Northwest European shelf.

Table 1: Changes from UKC3 to RCS-UKC4, note the default set-up in bold, the other options indicated in normal font are also available.

Parameter	**UKC3**	**RCS-UKC4**
Coupling frequency	1h	1h or **10mn**
Ocean model	NEMO3.6	NEMO4.0.4
Wave model	WAVEWATCH III v4.18	WAVEWATCH III v7.12
Atmosphere model	Unified Model v11.8	Unified Model v13.5
River model	None	River Flow Model (RFM)
Biogeochemistry	None	ERSEM
Atmosphere and Land configuration	RAL1 or **RAL2**	RAL1, RAL2 or **RAL3.3**
Cloud scheme	Smith, (1990)	Bi-modal (Weverberg *et al.*, 2021)
Microphysical parameterisation	Wilson & Ballard, (1999)	CASIM (Field *et al.*, 2023)
Runoff generation scheme	PDM	TOPMODEL
Soil hydraulics	(van Genuchten *et al.*, 1991)	Brooks & Corey (1964)

https://doi.org/10.5194/egusphere-2025-6216
Preprint. Discussion started: 20 January 2026

Non-penetrative fraction of light in ocean	0.66	0.58
Coupling terms Atmosphere to wave coupling terms	(Lewis et al., 2019a) u, v 10m wind	(Castillo et al., 2022) u, v 10m neutral winds
Ocean timestep	90s	90s or **60s** (with 10mn coupling)
Run mode	- MO-forecasts - MO-hindcasts	- MO-forecasts (near-real time) - MO-hindcasts - MO-ensemble forecasts - Climate hindcast

2.2 Run modes: deterministic, ensemble forecasts and climate runs

UKC3 could be forced by operational forecast lateral boundary conditions (LBCs) and initial conditions (ICs), either for past forecasts (MO-forecasts) or, when lateral boundary conditions were updated every day, to the global forecast started at midnight each day (MO-hindcast). This was limited to the period 2018-now, when individual components of the coupled system started to be operational (AMM15 ocean and waves).

The Regional Coupled System (RCS) was built to accommodate more complex ways of running the system:

- MO-forecasts (as in UKC3), additionally in UKC4 including the option to run near-real time forecasts initialised at 00:00UTC, where LBCs are picked from the operational suite on disk, rather than in the archiving system.
- MO-hindcast (as in UKC3), with LBCs reinitialised every day to the global forecast initialised at 00:00UTC for longer runs, used for short hindcast runs, e.g. days or months, option available from 2018, used in Berthou et al., (2024) and Partridge et al., (2025).
- MO-ensemble forecasts, based on the work from (Gentile *et al.*, 2022): 18-member ensemble integrating the Met Office Global and Regional Ensemble Prediction System over the United Kingdom (MOGREPS-UK, (Porson *et al.*, 2020)) atmosphere-land ensemble forecast with the regional ocean-wave system. The ensemble includes one unperturbed reference simulation and 17 perturbed members, where atmospheric initial and lateral boundary conditions are generated by downscaling perturbations from the global MOGREPS-G system. Each regional atmospheric perturbed member includes stochastic physics perturbations. While the atmospheric component is ensemble-based, the ocean and wave components start from the deterministic operational model, with coupling handled consistently across all members. Additional SST and land temperature perturbations are applied following (Tennant & Beare, 2014). SST perturbations are applied from MOGREPS-G SST perturbations through the OASIS coupler, and only seen by the atmospheric system, they are kept fixed for the whole forecast and they are applied so that their average across all ensemble members is 0, their maximum amplitude is 2°C.
- Climate hindcast (driven by ERA-5 in the atmosphere (Hersbach *et al.*, 2020), GloSea5 in the ocean (MacLachlan *et al.*, 2015) and an ERA-5 driven global Met Office wave standalone hindcast for the waves, similar to (E.U. Copernicus Marine Service Information (CMEMS) Wave physics reanalysis, 2025).

https://doi.org/10.5194/egusphere-2025-6216
Preprint. Discussion started: 20 January 2026

- Climate projections (driven by a global climate model, but not documented in this paper)

Known Good Outputs (KGO) have been added as benchmarking cases to ensure new changes in the Regional Coupled System do not break capability. Optimisation tests have been run to reach a balanced system with individual components running at the same speed.

2.3 Evaluation strategy

The evaluation strategy of the coupled system is split between different run modes, mixing weather, climate, atmosphere, river, ocean and wave evaluation strategies. The aim of this evaluation is to:

- characterize the impacts a new atmospheric configuration (Bush et al. 2025) has on the ocean (1-month long marine heatwave MO-hindcasts, 4-year climate hindcast: 2000-2003, Table 2). The two chosen marine heatwave cases (June 2023 and May 2024) are stratification extremes (Berthou *et al.*, 2024), which are ideal for evaluating the quality of the atmospheric radiative forcing, whereas the 4-year hindcast characterises average model biases and possible drift.
- evaluate feedback of coupling on 10m wind speed through winter ensemble forecasts
- evaluate river discharge in 4-year hindcast simulations
- evaluate the performance of the coupled system for ensemble wave forecasting (significant wave height) and ensemble atmospheric forecasting (1.5m temperature spread) (summer and winter 2023 near-real time ensemble forecasts, Table 2).
- evaluate the changes brought in by 10mn frequency coupling instead of 1h, particularly to enable the representation of meteotsunami (sensitivity tests on summer 2023 forecasts and additional 3-day MO-hindcast of a meteotsunami event on 01-11-2021).

We performed two near-real time ensemble trials: one in winter 2023 and one in summer 2023. Winter 2023 was characterized by cold and anticyclonic weather regimes in January cases and one named storm (Larisa) in March in the English Channel. The summer ensemble was run weekly every Monday during the Wescon field campaign in the UK (Barrett *et al.*, 2021), from June 5th to August 21st. The month of June was characterized by weak synoptic forcing: anticyclonic regimes for the first two weeks and weakly cyclonic regimes in the last two weeks. Exceptionally strong sunshine and weak waves generated an intense and long (1-month) marine heatwave over the Northwest European shelf (Berthou et al., 2024). The month of July and first two weeks of August were dominated by strong cyclonic circulation, with three named storms: Patricia, Antoni and Betty. The last two weeks of August had weaker circulation and a few sea breeze days.

https://doi.org/10.5194/egusphere-2025-6216
Preprint. Discussion started: 20 January 2026

185

Date	Atmosphere/Land config.	Notes
MO-ensemble forecasts (near real-time)		
13/01/23	RAL2, RAL3.2	Strongly cyclonic
16/01/23	RAL2, RAL3.2	Arctic air outbreak
23/01/23	RAL2, RAL3.2	British Isles anticyclone
30/01/23	RAL2, RAL3.2	Azores and then British isles anticyclone, weak westerlies
20/02/23	RAL2, RAL3.2	Azores high, weak westerlies
06/03/23	RAL2, RAL3.2	Strongly cyclonic: storm Larisa
05/06/23	RAL3.2	Scandinavian blocking: marine heatwave pre-conditioning
12/06/23	RAL3.2	Scandinavian blocking: marine heatwave build-up
19/06/23	RAL3.2	Weakly cyclonic, stable Marine heatwave
26/06/23	RAL3.2	Weak westerlies, stable Marine heatwave
03/07/23	RAL3.2	Strongly cyclonic: storm Poly, end of marine heatwave
10/07/23	RAL3.2	Weak westerlies
17/07/23	RAL3.2	Weak westerlies Next cases adopted increased penetrative light fraction
24/07/23	RAL3.2	Moderately cyclonic
31/07/23	RAL3.2	Strongly cyclonic: Storm Patricia
02/08/23	RAL3.2	Strongly cyclonic: Storm Antoni
07/08/23	RAL3.2	Strong southerlies
14/08/23	RAL3.2	Scandinavian blocking
16/08/23	RAL3.2	Scandinavian blocking, then Storm Betty
28/08/23	RAL3.2	Weak synoptic forcing
MO-hindcasts		
31/10/21 - 02/11/21	RAL3.3	Meteotsunami
01/06/23 - 05/07/23	RAL2, RAL3.2, RAL3.3	Marine heatwave
01/05/24 - 07/06/24	RAL2, RAL3.2, RAL3.3	Marine heatwave
Climate hindcast		
01/01/99- 31/12/03	RAL3.3	1999 discarded as spin-up year

Table 2: Experiments run for model evaluation

https://doi.org/10.5194/egusphere-2025-6216
Preprint. Discussion started: 20 January 2026

3 Improving model components

3.1 Impacts of changing the atmosphere and land configurations on the coupled system

3.1.1 Performance in marine heatwave conditions

Surface marine heatwave conditions are a good test-case for coupled systems: they often show an extreme stratification at the ocean surface, which means the ocean mixed layer is very shallow (Berthou *et al.*, 2024). Any error in the heat flux budget will translate into a large SST error. Therefore, we tested the change of atmospheric configuration on two recent marine heatwaves (June 2023, May 2024). The new atmospheric configuration (RAL3.3) leads to warmer SSTs than RAL2, with clear improvements for May 2024, and a shift from a cold (down to -0.5°C) night-time SST bias in June 2023 to a warm (up to 0.3°C) bias averaged over the northwest European shelf (Fig. 2). Note that the Operational Sea Surface Temperature and Ice Analysis (OSTIA) is a foundation SST product (Good *et al.*, 2020), so it should be compared to the model's minimum diurnal temperature. The additional cloud/microphysics tuning between RAL3.2 and RAL3.3 is beneficial in June 2023 but has little impact in May 2024. The main difference in SST in June between model versions comes from a difference in shortwave radiation, as further changes were implemented to increase stratocumulus cloud cover in anticyclonic conditions, judged too low in RAL3.2 by forecasters (Bush *et al.*, 2024). In May, the RAL3.2 to RAL3.3 cloud/microphysics tuning showed little impact on shortwave radiation, potentially because conditions were not as favourable for stratocumulus formation.

Because of the limitations of satellite SST products (limited by cloud cover, and night-time surface temperatures), we complement this analysis with a comparison of RAL2 and RAL3.3 against in-situ ocean temperature observations, usually taken at 0.5m depth, which is consistent with the first model level of AMM15. Figure 3 shows the average bias against in-situ SST observations available in the Met Office observation archive (including ships, buoys and sea platforms) for May 2024 and June 2023. This figure confirms the tendency of RAL2 to have a cold bias, and for RAL3.3 to reduce this bias: it is clear in May 2024 (Fig. 3b,d) and in the Channel and Southern North Sea in June 2023, though RAL3.3 shows a warm bias in the Northeast Atlantic, the Celtic Sea and the North Sea in June 2023 (Fig. 3a,c). Nevertheless, even in places where RAL3.3 degrades from RAL2, the warm bias in June 2023 rarely exceeds 1.5°C. Figure 4 shows the impact on 1.5m air temperature: RAL3.3 is mostly an improvement over RAL2, with the exception of the Celtic Sea and west of Scotland in June 2023. It is interesting to note that despite the warm sea surface bias in part of the domain in June, the air temperature still has a cold bias, in the North Sea, the Irish Sea and the Channel. In this particular marine heatwave, the atmospheric boundary layer was very shallow. This cold air bias suggests sensible heat fluxes may be too weak in RAL3.3 in low wind conditions. This point will need assessing in future model development.

Because of these results, the light penetration (66% of radiation applied to the first model level, and 33% penetrating deeper in UKC3) was tuned back to 58% applied to first model level, 42% penetrating (RCS-UKC4). This cooled the SST by ~0.2°C in the June 2023 marine heatwave (not shown). This light penetration value is now the same as the operational AMM15 model

https://doi.org/10.5194/egusphere-2025-6216
Preprint. Discussion started: 20 January 2026

(Tonani *et al.*, 2019b). Note that this value is spatially and temporally homogeneous, which is unrealistic, given the difference in ocean colour between turbid river plumes and tidal regions, "greener" phytoplankton bloom season and "bluer" winter/summer season. Using a time and space varying light treatment is planned in a future release (e.g. feedback from ERSEM to NEMO, as in Skákala et al. (2022)).

Overall, the evaluation of the regional coupled system in marine heatwave conditions pointed to RAL3.3 as configuration of choice regarding its total radiative budget when the mixed layer is shallow – although no direct measurement of the heat budget was made over the sea, SST is a good proxy for it during marine heatwave conditions because of the extremely shallow ocean mixed layer (Berthou *et al.*, 2024). Thanks to these results, the coupled system contributed, for the first time, in the decision for one more iteration in the development cycle next standard regional atmosphere and land configuration, from RAL3.2 to RAL3.3 (Bush *et al.*, 2024).

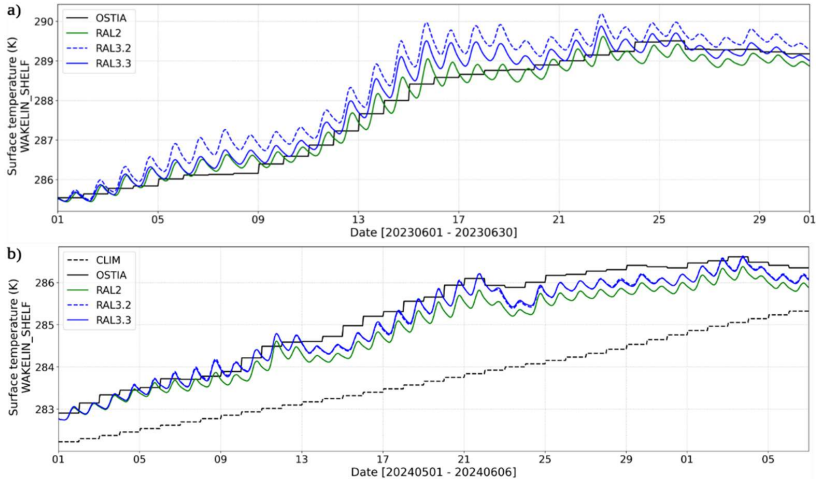

Figure 2: Sea surface temperature averaged over the Northwest European shelf for a) June 2023, b) May 2024 (01-05-2024 to 06-06-2024) in OSTIA, its 1982-2012 climatology, and the coupled system with RAL2, RAL3.2 and RAL3.3 atmospheric configurations.

https://doi.org/10.5194/egusphere-2025-6216
Preprint. Discussion started: 20 January 2026

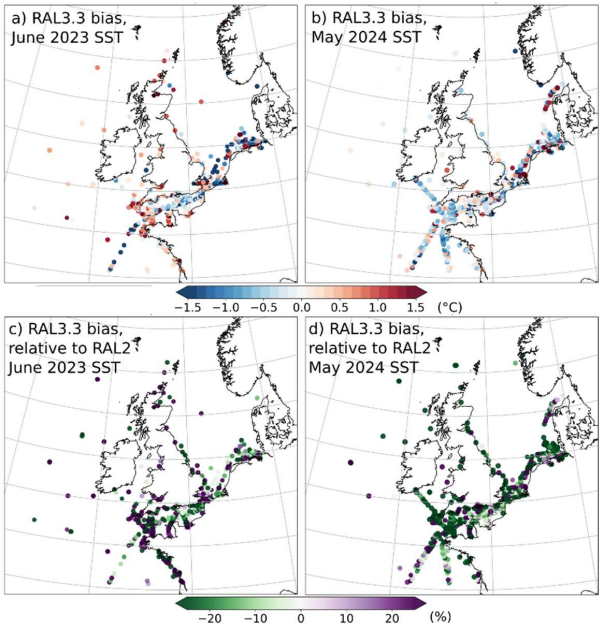

Figure 3: Mean sea surface temperature bias against in-situ ships and buoys averaged over the month of June 2023 (a) and May 2024 (b). Bias improvements from RAL2 to RAL3.3 (%) (c, d). Observation only used if recording more than 10 values over the simulation time.

https://doi.org/10.5194/egusphere-2025-6216
Preprint. Discussion started: 20 January 2026

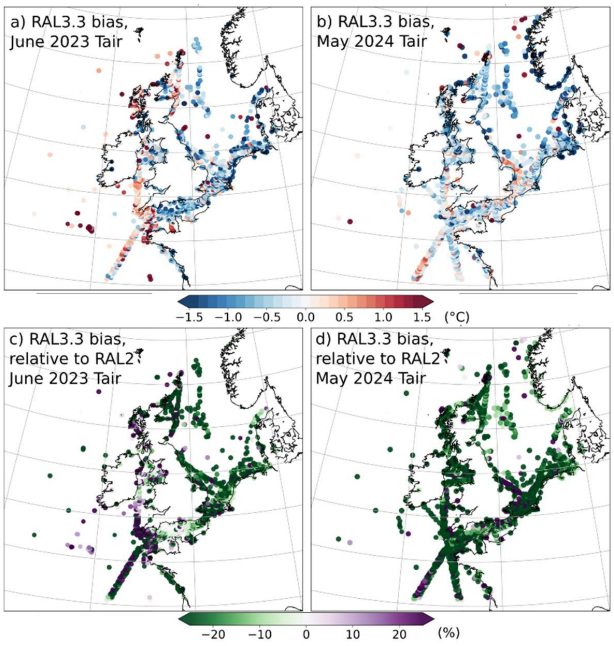

Figure 4: Same as Fig. 3 for 1.5m air temperature.

3.1.2 SST evaluation of UKC4 in climate simulations

Testing RAL versions on marine heatwaves has been useful to find the configuration with the best atmospheric radiative budget. However, evaluating multi-year simulations is essential for a coupled system, as any seasonal cycle imbalance in surface fluxes can bring large model biases or induce year-to-year drift in SST: we evaluate the quality of the sea surface temperature in 4-year long simulations. For such long simulations, the SST quality will both depend on the atmospheric fluxes and the ocean dynamics. Figure 5 shows that the 4-year mean bias in all seasons is always smaller than 1.5°C. Spring and summer show smaller biases (0.09-012°C), while autumn and winter have a warm bias of around 0.16-0.25°C. This warm bias persists throughout the seasons in the northwest part of the domain, where the ocean is deep. It is clear from these figures that the coupled system generates abundant fine-scale detail near coastal regions, but we cannot evaluate if these features are correct with low-resolution satellite-based SST products such as HadISST or even OSTIA. In the autumn, ocean cooling is dominated by entrainment and latent heat cooling, both related to wind speed: this autumn bias may be linked to an underestimation of the strongest wind speeds in UKC4 (see section 4): the cooling episodes of October-December are not strong enough, though the warm bias eventually disappears at the coolest stage (February-April). Nevertheless, the results indicate acceptable biases for the SST for a free-running coupled system. The biases do not grow over time, which is also a sign of good quality. Further

https://doi.org/10.5194/egusphere-2025-6216
Preprint. Discussion started: 20 January 2026

evaluation of this climate run will be done in a future paper, but this preliminary evaluation shows the RCS-UKC4 configuration is acceptable for both forecasting and climate modelling of the SST.

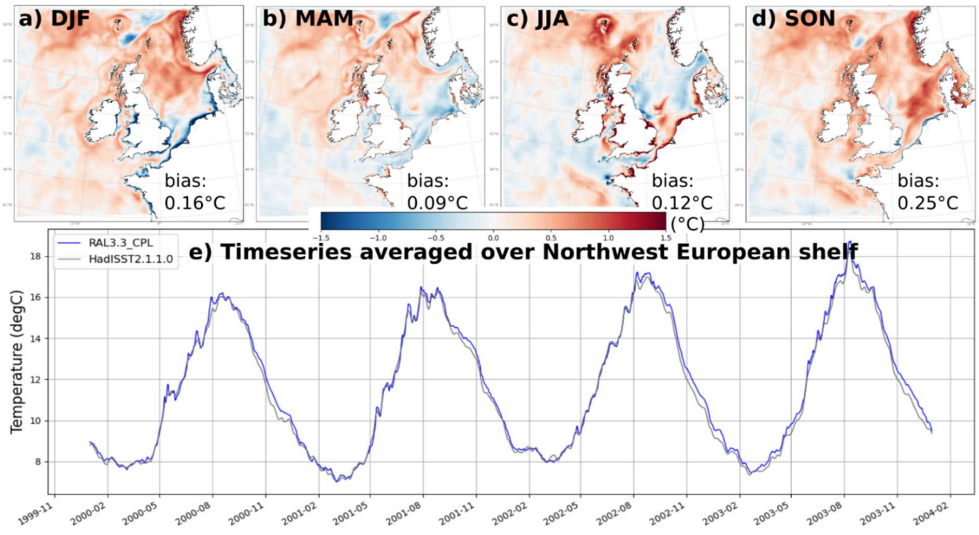

Figure 5: Sea surface temperature of the hindcast run (2000-2003) for ERA5 (= HadISST) and coupled model, a) averaged over December-February 2000-2003, b) averaged over March-May, c) June-August, d) September to November and e) averaged over the Northwest European shelf .

https://doi.org/10.5194/egusphere-2025-6216
Preprint. Discussion started: 20 January 2026

3.1.3 Changes in wind speed

In this section, we evaluate the wind speed changes brought by coupling over the sea in different weather conditions over the winter. Note this section uses ensemble forecasts in winter 2023 with RAL2 (uncoupled) and RAL3.2 (uncoupled and coupled). These results are expected to still be valid with RAL3.3: the microphysics/cloud tuning from RAL3.2 to RAL3.3 is not likely to impact wind speed, the rest of the section will refer to RAL3.

Gentile et al., (2021) documented a 10-20% wind decrease when coupling to waves in stormy conditions compared to uncoupled RAL2. They explained that part of this effect was due to different drag parameterisations between RAL2 and WAVEWATCH III source-term 4 (WWIII-ST4), as highlighted in Figure 6a: the drag coefficient relationship with wind depends on the Charnock coefficient and atmospheric stability functions. This relationship is steeper in WWIII-ST4, for which Charnock increases with wind speed faster than in RAL2, which uses a constant Charnock value. This difference resulted in a tendency of a wind decrease in coupled simulations, in particular in cases with strong winds. Gentile et al., (2022) recommended to upgrade the drag scheme to COARE4.0 with Donelan cap, which was adopted in RAL3, and is closer to the WWIII-ST4 parameterisation. Comparing wind biases against observations for RAL2, RAL3 and UKC4 in Figure 7 highlights that UKC4 is indeed closer to RAL3. We note little difference between RAL2, RAL3.2 and UKC4 in the 23/01/23 case, dominated by weak wind conditions, which is consistent with little differences in the drag at low wind speeds (Fig. 6a). In all the other cases, characterised by stronger wind speeds, the biases are better centred around 0 with RAL3 and UKC4 compared to RAL2, with reduced positive biases but sometimes enhanced negative biases. This illustrates that changing the slope of the drag/wind relationship has larger impacts than coupling. Nevertheless, the main effect of coupling is to enhance the spread around the drag/wind speed relationship, by introducing a wave-state dependency, as illustrated in Fig. 6a: the coupled system can have a larger variety of drag values for a given wind speed: waves can be in a growing or decaying state. This is particularly important around complex coastlines, where coastline reflection and sheltering effects mean the wave state is not always in equilibrium with the wind state.

The remaining difference in drag coefficient/wind speed relationship and the change in spread brought by coupling is still noticeable in probability of wind speed in ensemble forecasts (Fig. 6). At moderate wind speeds (illustrated in Fig. 6b, c), coupling with waves has the same effect as reported in Gentile et al., (2022): young, growing waves extract momentum from the atmosphere and reduce the wind speed, in particular in the sheltered North Sea. This is illustrated well by Fig. 6a, where the spread in the drag is increased towards higher values compared to atmosphere-only for 10m/s values. At storm-force wind speeds (20m/s), the probability of reaching such wind speeds in coupled mode (Fig. 6d, e) is slightly higher, as in some regions the drag coefficient is lower with waves for these wind speeds (Fig. 6a). The reduction of moderate wind speeds with wave coupling over the sea has an impact on coastal winds, with a ~0.1 to 0.2m/s reduction in ensemble mean wind speed in all four cases (not shown).

https://doi.org/10.5194/egusphere-2025-6216
Preprint. Discussion started: 20 January 2026

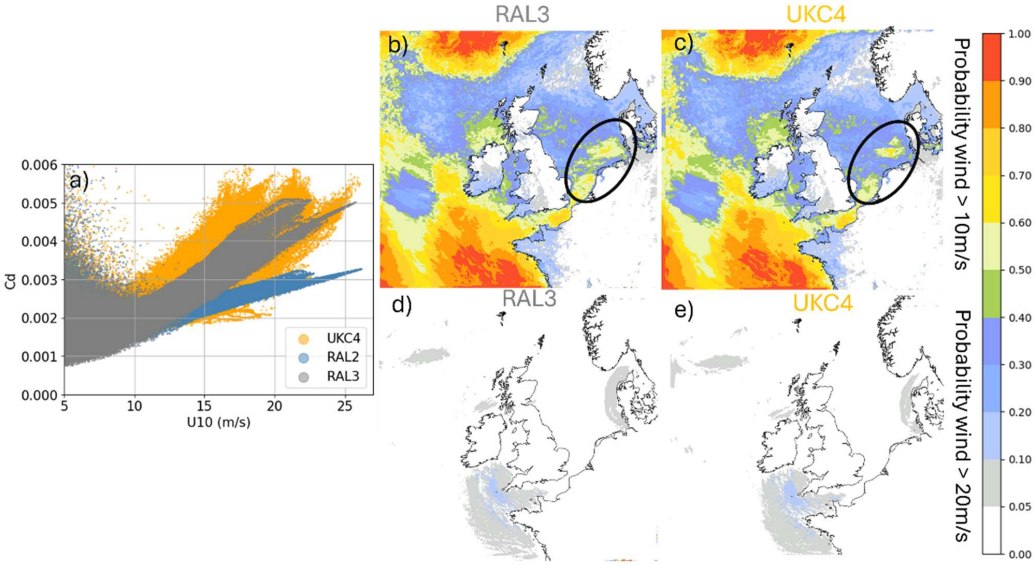

Figure 6: Probability of wind speed > 10m/s (a, b), >20m/s (c, d) for atmosphere only with RAL3.2 configuration (a, c), atmosphere-ocean-waves with RAL3.2 (b, d). e) shows the drag coefficient as a function of wind speed for RAL3 (atmosphere-only), Waves – ST4 terms (active in coupled system) and RAL2.

https://doi.org/10.5194/egusphere-2025-6216
Preprint. Discussion started: 20 January 2026

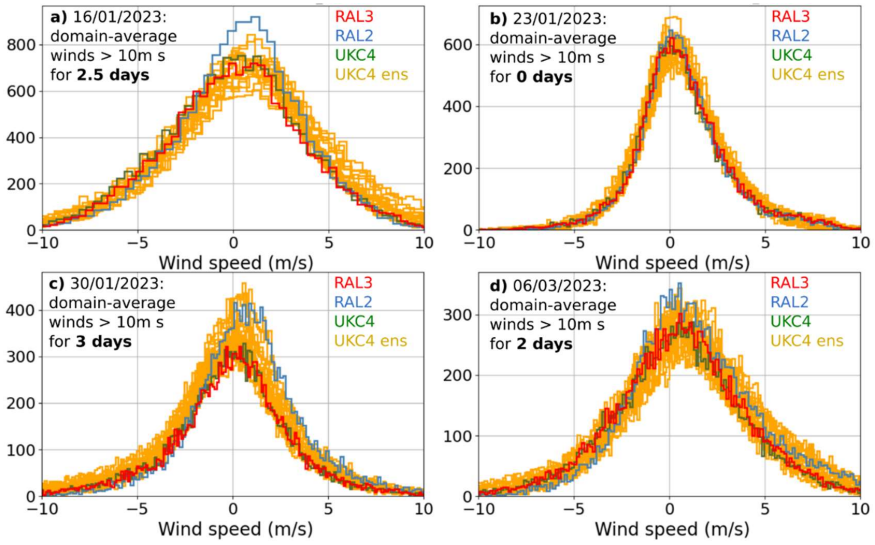

Figure 7: Histogram of wind biases against all buoys for four different winter 2023 cases, an indication of duration of strong wind speeds averaged over the sea part of the domain is given on each figure (length of time when at least a few members reach a domain-average mean wind speed of 10m/s).

3.2 Quality of the river flows

Following Lewis & Dadson (2021), hereafter LD2021, rivers have been added to the regional coupled system. River routing uses the River Flow Model (see Appendix B of Lewis et al., (2018)). The JULES configuration has been upgraded since LD2021 and a main difference is the runoff generation scheme, which changed from the Probability Distributed Model (PDM, (Moore, 1985)) in LD2021 to the 1D groundwater model TOPMODEL (Gedney & Cox, 2003) in the RAL3 configuration used in RCS-UKC4. In both configurations, a saturation excess runoff is calculated by JULES, increasing with rainfall intensity (Best et al., 2011). In addition to this, PDM and TOPMODEL calculate additional surface and subsurface runoff. In PDM, additional surface runoff depends on the saturation of the first two layers of soil. Subsurface runoff is calculated by JULES as water drainage at the bottom of soil layer 4. In TOPMODEL, surface runoff is a function of whole soil column saturation and local topographic variability. Subsurface runoff depends on water content below the calculated water table depth, and a topographic index, which relates to the upstream area draining into a locality and the local slope. In general, PDM tends to generate more surface runoff, while TOPMODEL generates more subsurface runoff. The River Flow Model then routes surface and subsurface runoff with different wave speeds: $0.5m\ s^{-1}$ for surface runoff and $0.05m\ s^{-1}$ for subsurface runoff. This is constant across the whole of the UK.

https://doi.org/10.5194/egusphere-2025-6216
Preprint. Discussion started: 20 January 2026

Figure 8 shows evaluation metrics of the daily model flow against the National River Flow Archive (NRFA) gauges. Matching was done based on nearest neighbour maximum flow at NRFA gauge location using closest point to location and its surrounding 8 grid points. Nash-Sutcliffe efficiency (NSE) shown in Figure 8b is the ratio of RMSE to observation variance. Negative values mean model has worse skill than prediction based on average observed flow, values above 0 show model has skill in both mean and variability, and values close to 1 show perfect model. NSE is negative in most of the UK Southeast and in the west of Scotland, whereas it ranges from 0.2 to 0.8 in the southwest and north of the UK. To understand the model performance, we further show the three components of the Kling-Gupta efficiency: normalised bias, ratio of model and observation variances, and Pearson correlation coefficient in Figure 8a,c,d. The bias shows a variable pattern with no clear spatial pattern emerging. However, the ratio of variance clearly shows an overestimation of flow variability in the UK Southeast and western Scotland and an underestimation in the southwest, west and north of the UK. Similarly to NSE, the correlation between observed and modelled flows is close to 0 in the southeast, and is closer to 0.4-0.8 in other parts of the UK. Southeast UK catchments are usually connected with aquifers and have long time-responses: they are dominated by baseflow. In other regions, catchments are flashier, with faster response. This is illustrated in Figure 9, which shows the largest UK catchments, on the left from catchments in the west of the UK, from south to north from bottom to top, and similarly for catchments in the east on the right hand side of the figure. The catchments in the west and north show too much baseflow, and underestimated extreme values. They show too small an amplitude of the annual cycle, with underestimated winter peaks, and overestimated summer peaks, while the two southeast catchments show too much variability and not enough baseflow. This shows that TOPMODEL tends to keep too much water locked in the soil in winter, slowly released as baseflow in spring and summer in the west and north of the country. In these regions, soil is not always as deep as 3m, as assumed by JULES: Weedon et al., (2023) recommend reducing saturated conductivity to very low values in deeper parts of the soil in these areas, which would reduce soil capacity to store water. Weedon et al., (2023) also showed that JULES with TOPMODEL showed too much surface runoff in the UK Southeast, and recommends using large values of saturated conductivity, based on bedrock properties rather than soil properties. This will be tested in future model releases. In addition, testing of spatially-variable river speed should be done, as recommended by Lewis et al., (2018).

https://doi.org/10.5194/egusphere-2025-6216
Preprint. Discussion started: 20 January 2026

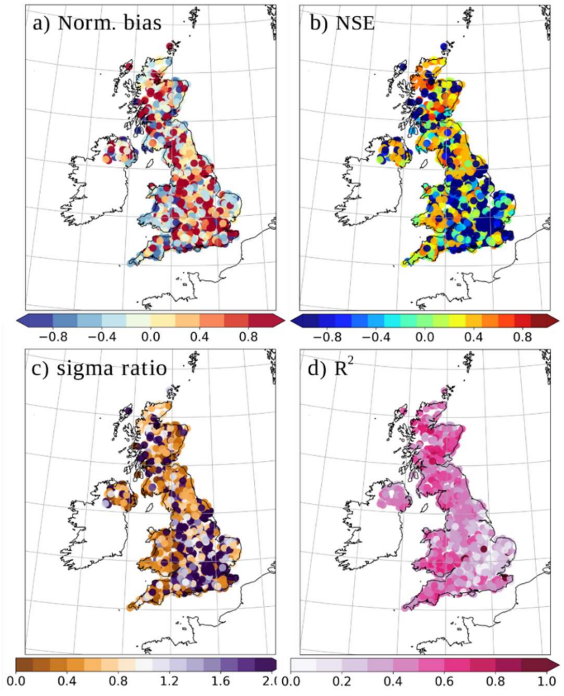

Figure 8: River discharge statistics against NRFA gauges: a) normalised bias: Model/Observations, b) Nash-Sutcliffe efficiency, c) variance ratio (model/observations), d) Pearson correlation coefficient. Note a), c) and d) are the three components of Kling-Gupta efficiency.

https://doi.org/10.5194/egusphere-2025-6216
Preprint. Discussion started: 20 January 2026

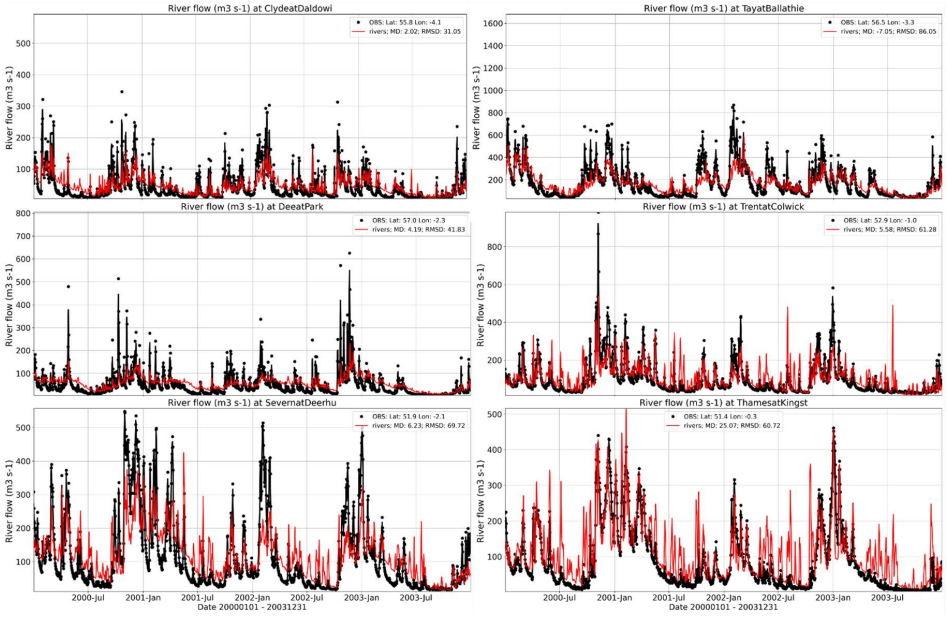

Figure 9: River discharge in the six largest catchments of the United Kingdom, using the gauge closest to the sea (note this can still be >50km from the sea).

4. Introducing ensemble components

This section demonstrates the ensemble forecasting capability of RCS-UKC4, with a particular focus on waves, winds and ensemble spread of air temperature.

4.1 Quality of the ensemble wave forecast

We first analyse the quality of Significant wave Height (HS) and 10-meter Wind Speed (WS) for 5-day MO-ensemble forecasts for the cases shown in Table 2, which include five storms. The analysis is done for day 3 of the forecast, as this is the critical period for using regional ensembles to accurately predict hazards and improve forecasting (Porson *et al.*, 2020). A storm is defined as an event when named by the Met Office or another agency, which means it had significant hazards associated with it, in these cases associated with strong wind speeds. We compare UKC4 ensemble forecasts with the current operational Atlantic wave ensemble. The operational Atlantic wave ensemble is an uncoupled wave model (WWIII) that has a domain covering the whole Atlantic basin with a multi resolution cell structure allowing higher resolution over the UK (3km). It is driven by the current operational global atmosphere only ensemble MOGREPS-G (Valiente *et al.*, 2023).

The spatial distribution of the buoys used for measuring HS, WS, and SSTs are shown in Figure 10. There is a clear concentration bias in HS and SST near the coast and oil rigs in the North Sea, while the WS measurements show a concentration

https://doi.org/10.5194/egusphere-2025-6216
Preprint. Discussion started: 20 January 2026

bias primarily around the oil rigs in the North Sea. Coastal buoys around the UK were excluded from the wind speed analysis because their measurements over the time period considered were infrequent and unreliable.

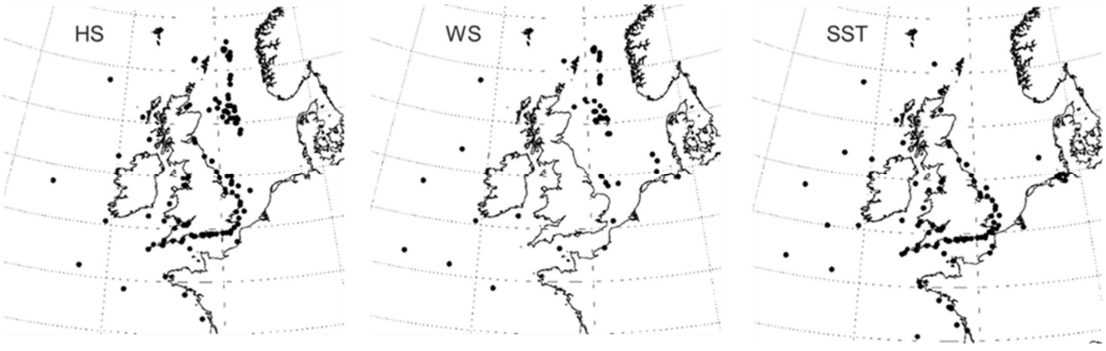

Figure 10: Location of the buoys used for measuring HS (left), WS (centre), and SSTs (right) are shown. The figure presents the domain and locations of all the buoys used for each variable, marked with dots.

4.1.1 Wave Ensemble Forecast

Evaluating ensemble skills ensures that the forecasting system is robust and can effectively handle uncertainty in variable mid-latitude weather conditions. When evaluating the reliability of an ensemble prediction system, the Root-Mean-Square Error (RMSE) of the ensemble mean is commonly compared to the average ensemble spread, calculated as the square root of the average ensemble variance (Fortin *et al.*, 2014). Figures 11 and 12 include the bias, RMSE and ensemble spread of HS and WS for six cases. The RMSE excludes any observational error: we expect that a good ensemble has a spread to RMSE ratio slightly greater than one. UKC4 exhibits promising and comparable forecasting skills for both HS and WS when compared to the Atlantic operational wave ensemble. UKC4 is a competitive candidate for HS forecasting: during storms, it often outperforms the operational ensemble in terms of bias, with up to 90% bias improvement for the Patricia case study (31/07/23), the improvement is seen in the growing phase of wave development, though the decaying phase tends to be degraded by UKC4 by 20%. However, during more settled weather conditions, UKC4 generally becomes less accurate and overestimates HS, typically worsening the bias by about 20%.

Nevertheless, the RMSE for UKC4 typically provides a continuous improvement for HS throughout the 5-day forecast of around 10% compared to the operational ensemble. The improved RMSE in the coupled system is most likely due to the combination of increased resolution and the wind and wave modulation by tidal currents, which are particularly strong in the English Channel, Southern North Sea and Irish Sea, where most of the buoys are located. Indeed, tidal currents change direction every 6h and reach about 1m/s. Waves are amplified when they propagate against the current and dampened when they propagate in the same direction, resulting in the oscillations seen in the timeseries of a buoy in the English Channel (Fig. 13).

https://doi.org/10.5194/egusphere-2025-6216
Preprint. Discussion started: 20 January 2026

Winds are also modulated by tidal currents (Renault & Marchesiello, 2022), which further modulates waves. This figure demonstrates the positive impact of coupling on forecasting HS in a tidally active area. UKC4 accurately represents the oscillations, particularly during and after the storm from 02/08/23 to 05/08/23. Tidal currents can amplify large waves during storms, as shown at 22:00UTC on 02/08/23, with a wave peak at 2.6m, captured in the regional coupled system spread. In contrast, the operational ensemble does not show any oscillation, hence a larger RMSE and wrong timing of wave peak.

Regarding model spread (Fig. 11), there is no initial spread in HS for the regional coupled model as the initial condition comes from the deterministic operational marine ocean-wave model. Yet, the spread spins up to similar values to the operational ensemble in around 6 hours. After this, both models tend to be under-spread, with UKC4 being closer to a spread-to-error ratio of one than the operational system.

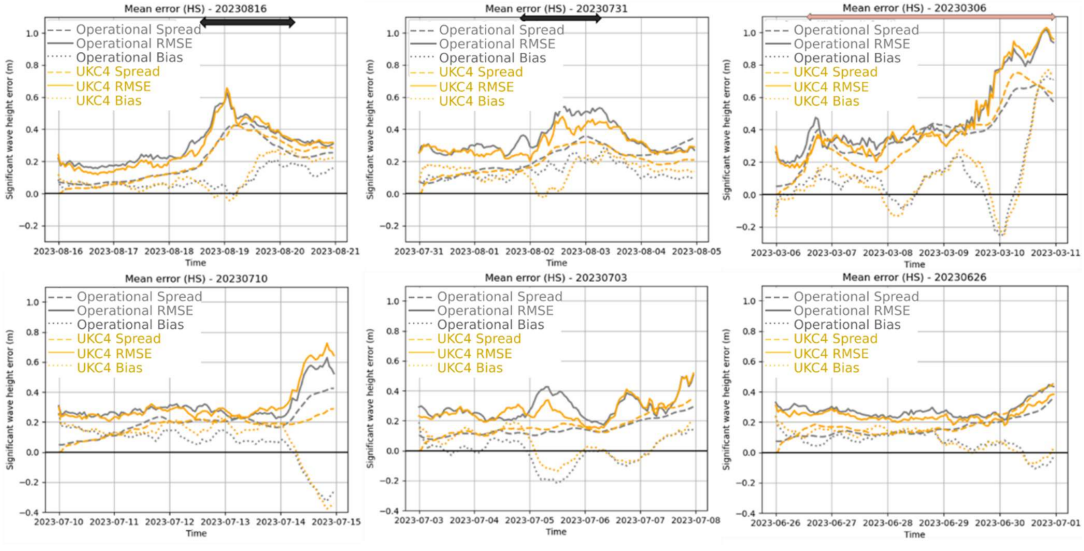

Figure 11: Mean ensemble bias (dotted lines), RMSE (solid lines) and spread (dashed line) for significant wave height (HS) averaged across all buoys shown in Fig. 9. UKC4 performance is shown in yellow, standalone operational wave ensemble in grey. Each panel shows a 5-day forecast in spring and summer 2023, including 3 storms (top row, indicated with double arrows).

https://doi.org/10.5194/egusphere-2025-6216
Preprint. Discussion started: 20 January 2026

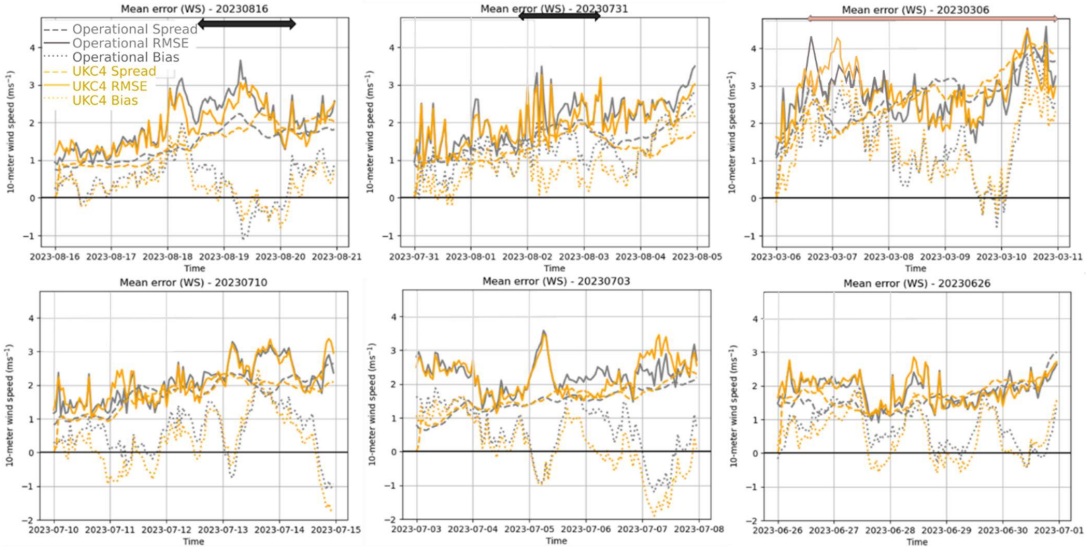

Figure 12: Same as Fig. 10 for wind speed (WS) using buoys shown in Fig. 9.

410

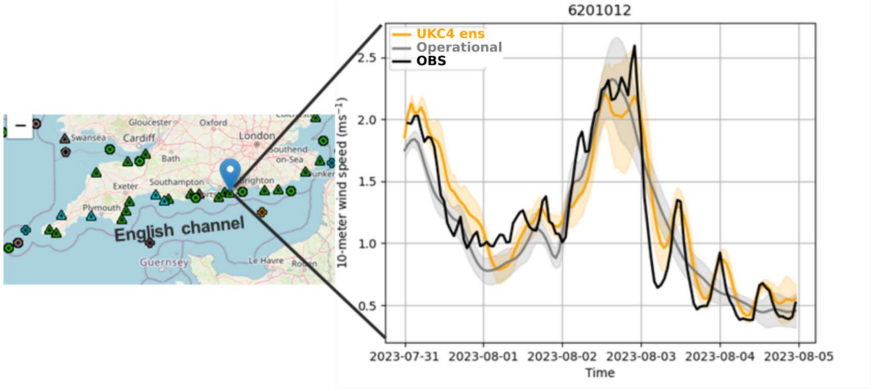

Figure 13: Impact of wave modulation by tidal currents in the English Channel. The regional coupled model (orange), Atlantic operational wave ensemble (grey) and observations (black), with the shaded area indicating one standard deviation from the mean ensemble bias.

415

In terms of wind speed, Figure 12 demonstrates that the UKC4 tends to improve the wind bias (~30%) through 5-day forecasts, with negligible improvements in the RMSE. It is important to note that this improvement in wind speed may not solely stem

https://doi.org/10.5194/egusphere-2025-6216
Preprint. Discussion started: 20 January 2026

from coupling but could also arise from the higher resolution and different scientific configuration of MOGREPS-UK compared to MOGREPS-G.

Overall, both models forecast the bulk of the distribution of HS and WS to a reasonable degree, with a typical RMSE of around 0.4m and 2m/s and a typical bias of around 0.1m and 1m/s respectively. Additionally, Figure 14 provides helpful summary density scatter plots, highlighting the model's ability to correctly represent the extremes as well as the main part of the distribution. These figures use the whole 5-day forecast and all the ensemble members of the Atlantic wave ensemble (a, c) and UKC4 (b, d) against the observations for all six cases together for HS (a, b) and WS (c, d). Both ensembles are well centred around the 1-1-line, re-iterating their general good quality. Both models tend to overestimate HS below 2m and underestimate them above it, with the same being true for WS except centred around 7.5m/s. This is a common problem in wave and atmospheric models (Wahle *et al.*, 2017; Valiente *et al.*, 2023). This tendency is slightly exacerbated in the coupled ensemble, potentially because individual models within the regional coupled model (UM, WWIII, NEMO) are finetuned to an uncoupled model configuration.

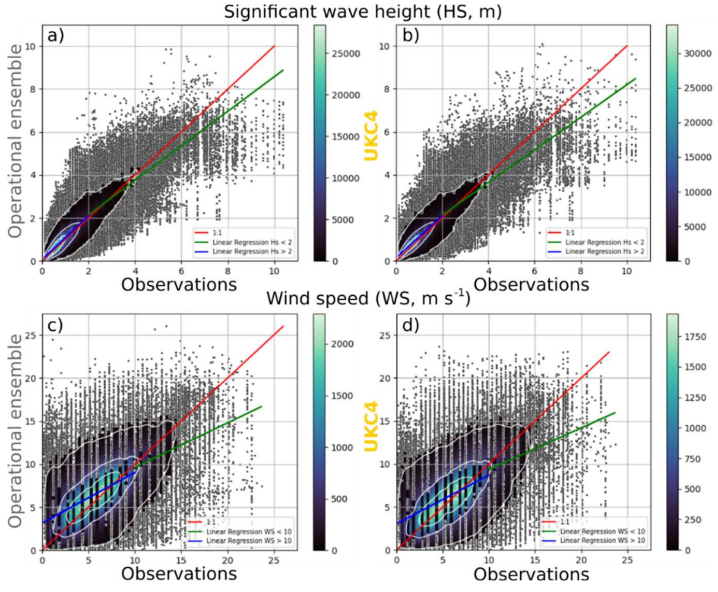

Figure 14: summary density scatter plots comparing the ensemble predictions against observations for all six cases across all buoys and all 5-day forecasts, covering the entire distribution of significant wave height (HS, a-b) and 10-meter wind speed (WS, c-d). The plots include a red one-to-one line, a blue linear regression for HS below 2m and WS below 10 m/s, and a green linear regression for HS above 2m and WS above 10 m/s. The left column depicts the Atlantic

https://doi.org/10.5194/egusphere-2025-6216
Preprint. Discussion started: 20 January 2026

operational wave ensemble, while the right column shows UKC4. Colorbar shows a fitted gaussian kernel density estimation.

4.1.2 Adjusting wind/wave coupling

The previous section showed improved wind biases in UKC4 in ensemble mode for the bulk of the distribution, though stronger underestimation of high WS compared to the global ensemble MOGREPS-G. However, the wave improvements were mostly found for higher wave height and for the RMSE rather than biases. This suggest that UKC4 can be further improved in its wind/wave interactions. Four sensitivity tests have therefore been conducted:

- Increasing the coupling frequency from 1 hour to 10 minutes
- Converting the wind speed sent from the UM to WW3 model from 10-meter winds to 10-meter neutral winds, as WW3-ST4 is assuming a neutral wind profile to interpolate winds to the surface
- Fine-tuning the wave growth parameter (Betamax)

These parameters are explained in detail in subsections below and the impact of these tests on HS and WS are analysed, with an additional focus on SSTs as a coupled system cannot afford to improve only one variable.

Impact of increasing the coupling frequency:

Increasing the coupling frequency from 1h to 10 minutes was intended to improve the diurnal cycle of SSTs and enable the representation and forecasting of meteotsunamis (Lewis *et al.*, 2023); the latter is investigated in section 5. Switching to 10mn coupling itself has no impact on the cost of the coupled system. However, the ocean timestep had to be reduced from 100s to 60s, because more frequent coupling led to decreased ocean model stability, which increased model cost.

Increasing the coupling frequency to 10 minutes shifts HS, WS and SST growth and decay forward in time (Fig. 15): by 1h in waves, and 2h for wind and SST. For waves, the forward lag is stronger when waves are growing, which is consistent with the fact that the winds will have stronger impacts on the waves when they are growing, as waves then extract kinetic energy from winds (Janssen, 2004; Ardhuin *et al.*, 2010). This leads to marginal improvements in wave and wind forecasts, though can generate too early wave growth as on 02/08/23 (Fig. 16). SST RMSE is consistently improved, particularly outside storm events, when a diurnal cycle develops. This is partly due to the correction in the delay introduced by external coupling, where fluxes generated by one model are waiting until the next coupling time step to be sent to the other model: they are only waiting 10mn when the coupling frequency is increased. However, this would only explain 50mn difference. The remaining difference is due to models adjusting to each other more frequently, being in closer equilibrium. Overall, increasing the coupling frequency improves SSTs and shows marginal improvements to wind and waves, and small deterioration in strong wave growth conditions.

https://doi.org/10.5194/egusphere-2025-6216
Preprint. Discussion started: 20 January 2026

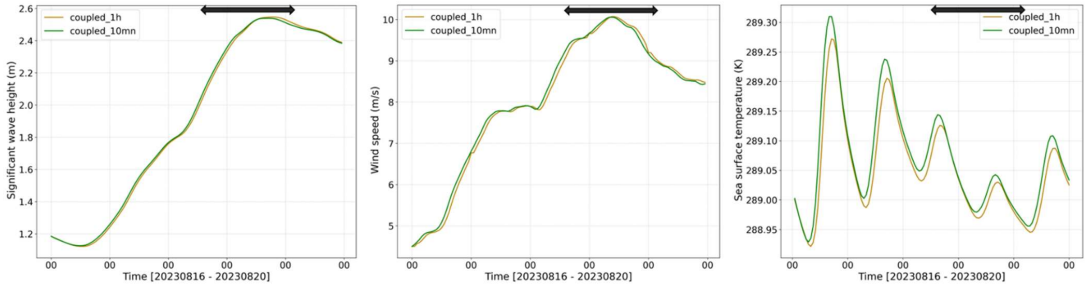

Figure 15: Domain-averaged timeseries comparison of UKC4 with 1h and 10mn coupling frequencies showing the mean HS (first column), WS (second column), and SST (third column) across the entire UK domain, storm Betty case study (16/08/2023). Coupling frequency: 1 hour (1 hour, currently in use), and 10-minute (green).

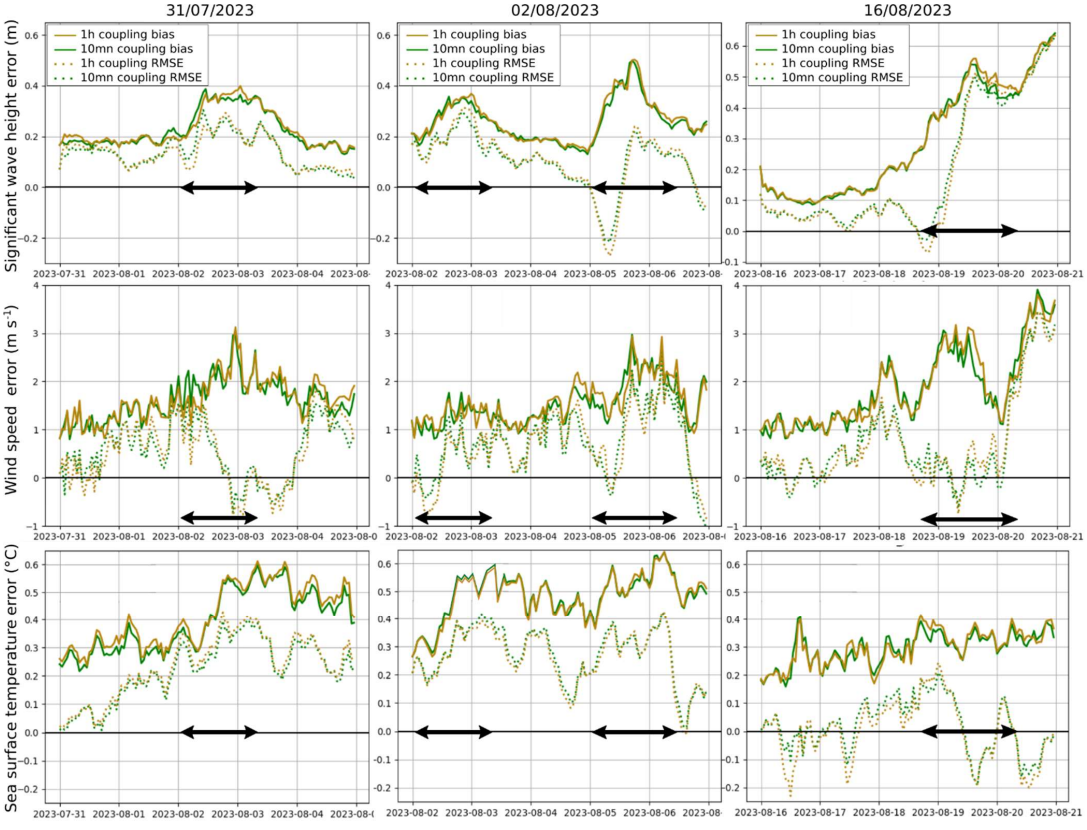

https://doi.org/10.5194/egusphere-2025-6216
Preprint. Discussion started: 20 January 2026

Figure 16: Three 5-day storm forecasts of 2023 spring and summer case studies, for HS (first row), WS (second row) and SST (third row). Comparing two different coupling frequencies; gold 1h and green 10-minute. The dotted lines represent the mean bias, and the solid line is the mean RMSE across all buoys through time. The black arrows indicate when the average WS across the whole domain exceeds 7.5m/s.

Changing wind/wave coupling parameter (Betamax)

The second sensitivity test involved changes in the growth parameter (Betamax). Betamax is a non-dimensional parameter that characterizes the maximum amount of energy exchanged between wind and waves. The four different Betamax parameters that were tested include 1.6 (Bidlot, 2020), 1.48 (1.48 in Met Office regional deterministic system driven by the European Centre for Medium Range Weather Forecasting winds, (Valiente *et al.*, 2023)), 1.39 (Met Office global Operational wave ensemble, (Valiente *et al.*, 2023) and 1.2 (Janssen, 1991) across three storm cases studies. Overall, using a reduced Betamax decreased the mean bias across buoys for HS, with the opposite effect on WS and SSTs (not shown). Because the reduction from 1.48 to 1.39 was judged to be minor, and the coupled system typically shows a warm SST bias, the value was kept at 1.48. These sensitivity tests illustrated that a balance has to be reached in a coupled system, where a parameter cannot be tuned for a single variable (e.g. HS) without checking the impact on other variables (e.g. WS and SST).

Passing Neutral Winds instead of Winds

When 10m wind speeds are sent to the wave model, it calculates surface wind speed using a logarithmic profile assuming a neutral boundary layer profile. Therefore, sending neutral wind speed from the atmosphere to the wave model enables a more consistent treatment of momentum in the coupled system. Results indicated localised impacts during storm cases, generally resulting in positive outcomes (up to 60% improvement for HS and 70% for WS for storm Betty, but closer to 5% improvements in other cases). Impacts on SST biases were of the order of 5% and case-dependent, with no systematic change. These wind and wave changes appear to be case study dependent with storms being highly complex with a variety of different boundary layer stability depending on storm sectors. Given the improvements in most cases for HS and WS, and the more consistent treatment of momentum transfer between models, this change was adopted in UKC4.

4.2 Impact of coupling on the atmospheric ensemble spread

For an ensemble to be judged of good quality, the model error should be similar to model spread, so that the observations are contained within model spread. The 1.5m air temperature biases can be substantial in atmospheric models: additional perturbations are applied to the sea surface temperature following Tennant & Beare (2014) to artificially enhance the spread in air temperature. These perturbations have a maximum amplitude of 2°C and generate greater variations where the climatological day-to-day fluctuations in SST are largest. However, this perturbation strategy was designed for global prediction systems and subsequently adopted in the regional ensemble.

https://doi.org/10.5194/egusphere-2025-6216
Preprint. Discussion started: 20 January 2026

We investigated what the impact of coupling on air temperature spread is when keeping these perturbations added to the SST field sent by the ocean to the atmosphere via the OASIS coupler. In a global coupled framework, (Lea *et al.*, 2022) found they could reduce the 2°C maximum perturbation amplitude to 1.8°C as coupling was able to provide a physically-meaningful 0.2°C spread. In RCS-UKC4 ensemble simulations, all the ocean and wave members are starting from the operational deterministic analysis of the ocean and wave models respectively. This is because regional ocean ensemble data assimilation is not yet mature enough to be included in the system, meaning that all spread generated in these components in coupled simulations are in response to the atmospheric spread in wind, and radiation.

Figure 17 shows the ratio of the standard deviation in surface temperature of UKC4 (coupled) and RAL3 (atmosphere-only) ensembles towards the end of the 5-day forecast (T+112) for the different cases run over summer 2023 and winter 2023. Positive values (red shading) indicate regions with increased spread in the coupled ensemble relative to the uncoupled (atmosphere only) ensemble. When apparent, increased ensemble spread tends to be largest around UK coastlines, however there is substantial spatial variability linked to each case-specific situation. Enhanced spread is largest and most widespread during the 05/06/2023 and 19/06/2023 summer cases when marine heatwave conditions were dominant, and record shortwave radiative forcing was present (Berthou *et al.*, 2024). In contrast, coupling has more limited impact on surface temperature spread in the winter, beyond local differences confined to near-coastal areas.

https://doi.org/10.5194/egusphere-2025-6216
Preprint. Discussion started: 20 January 2026

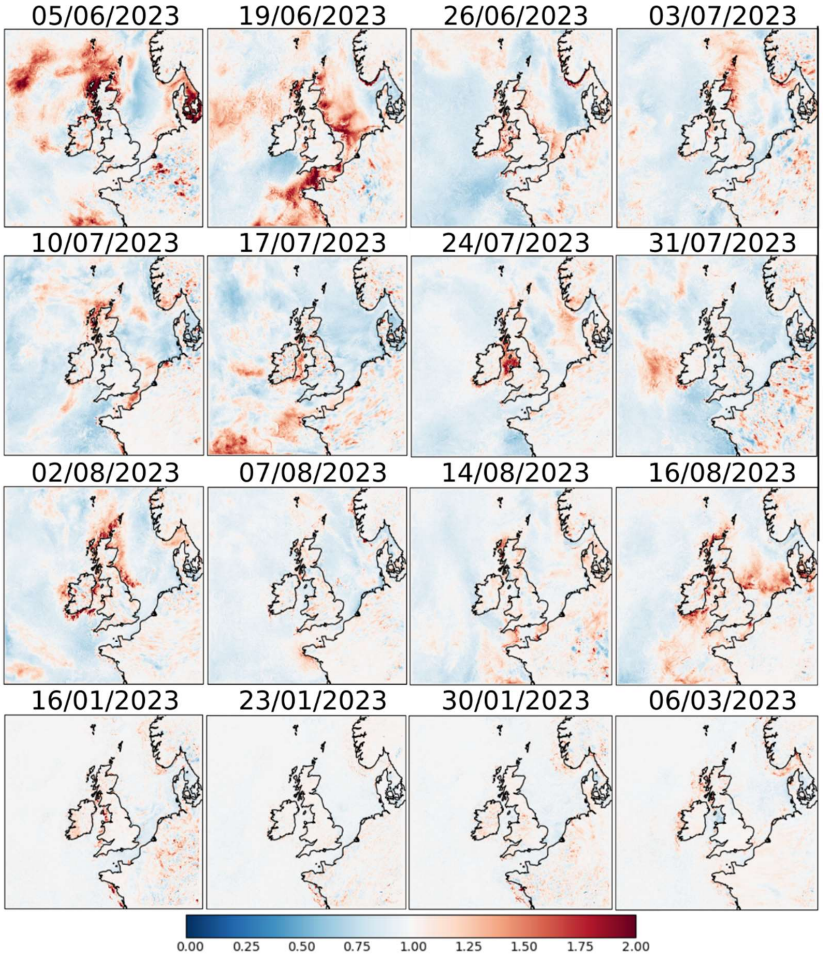

Figure 17: Map of standard deviation ratio between UKC4 (coupled) and RAL3 (atmosphere-land only) ensembles for surface temperature at T+112 of the forecast for the 12 cases run over summer 2023 and the 4 cases run over winter 2023. Greater than 1 (red colours) depicts regions where there is increased spread in UKC4 relative to RAL3. Less than 1 (blue colours) depicts regions where there is reduced spread in UKC4 relative to RAL3.

To understand the drivers of either relatively reduced or increased SST spread brought by the coupled system, we investigate whether the SST anomalies imposed in the atmosphere-only run generate a flux adjustment in the radiative or turbulent heat fluxes. Figure 18 shows the relationship between imposed SST anomaly and surface flux anomalies in each member for two summertime atmosphere-only ensemble simulations, with spatially averaged results for five hydrodynamically-consistent

https://doi.org/10.5194/egusphere-2025-6216
Preprint. Discussion started: 20 January 2026

ocean regions surrounding the UK (Fig 1b). Results for shortwave radiation fluxes show large spread between members, but no relationship to the SST anomalies, indicating that this spread originates from atmospheric drivers linked with variations in cloud cover between members. In contrast, a negative relationship emerges for the long wave radiative fluxes, sensible heat flux, and particularly for latent heat flux. Warmer SSTs generate negative flux anomalies towards the ocean, which in a coupled system will act to cool it. In UKC4, where the SST will respond to changes in radiative fluxes, the latent heat flux (and to a lesser extent longwave radiative flux and sensible heat flux) response to SST perturbations will tend to dampen the SST anomalies, therefore acting to decrease the ensemble spread. Only increases in random shortwave perturbations are likely to increase SST spread. Therefore, the coupled ensemble spread in SST is more likely to increase when cloud cover variability between members and shortwave radiative forcing are large, while spread in SST is likely to decrease in cases dominated by latent heat flux cooling.

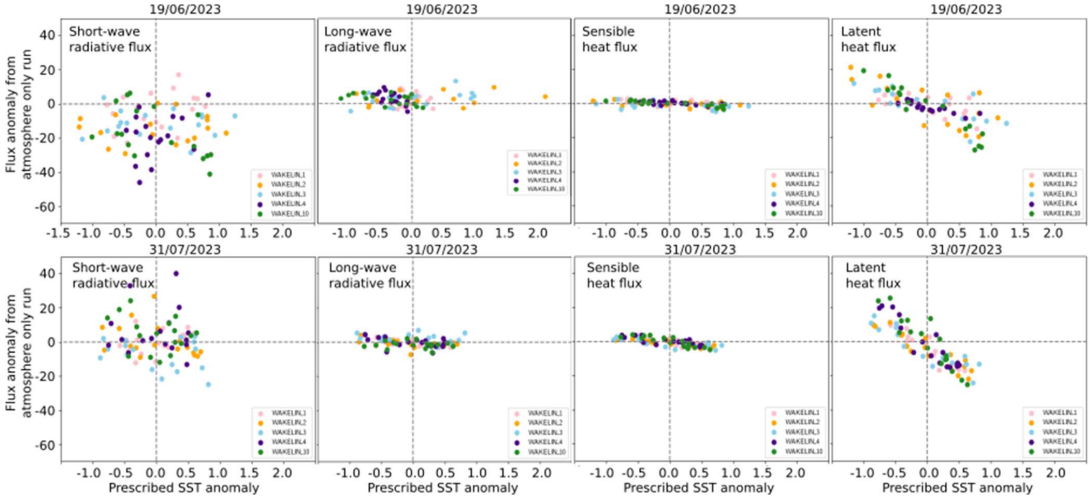

Figure 18: Scatter plots of flux anomalies (averaged over 5 days of the run) compared to SST anomalies (averaged over the last day) in the atmosphere-only ensemble. Top row is for the case initialised on 20230619 and bottom row is the case initialised on 20230731. First column shows SW heat flux anomaly, second column is LW heat flux anomaly, third column is sensible heat flux anomaly, and fourth column is latent heat flux anomaly. Each point is a member of the ensemble, and the different colours are Wakelin regions.

We now focus on explaining the difference in the magnitude of spread changes between cases, and in particular summer and winter. We show the relationship between net heat flux anomalies in the coupled system, versus SST anomaly growth or decay between UKC4 and RAL3 simulations in Figure 19. This relationship is usually positive, indicating that when a member has larger net fluxes into the ocean, the SST warms compare to the control, and vice-versa. However, the slope of the relationship varies between cases and regions: summer cases have a larger SST warming for similar flux differences, and the Irish sea, English Channel and southern North Sea (resp. Wakelin_9, Wakelin_4 and Wakelin_1) have smaller SST changes for similar

https://doi.org/10.5194/egusphere-2025-6216
Preprint. Discussion started: 20 January 2026

flux differences compared to other regions. Figure 19 also indicates the average SST change which would be expected by a simple mixed layer heat budget computed on the averaged mixed layer depth over the 5-days and for each region. Differences are consistent with the simulation results shown. Although a crude approximation therefore, the difference in mixed layer depth between winter and summer, between regions and cases largely explains the different SST response to flux differences. For example, the 19/06/2023 case has an extremely shallow mixed layer (~11-12m in the North Sea) and shows strongest changes in SST in the coupled system compared to atmosphere-only system. This is further supported by Wakelin 1 (Channel region) having a systematically steeper slope than the other regions in the SST/flux relationship. This area is permanently mixed vertically, with an average 30m depth, so that even large changes in flux result in small changes in SST. In winter, when the mixed layer depth is deep (48m and 78-80m in the central and northern North sea respectively (Wakelin_2 and Wakelin_3), close to the average depth of these regions, any changes in fluxes arising from coupled feedbacks have very little effect on the SST.

To conclude the section, UKC4 is likely to increase air temperature spread in summer cases with strong radiative fluxes and variability in cloud cover between members, but is likely to decrease it in conditions dominated by strong winds and latent heat fluxes. It is likely to have minimal impacts on spread in the winter.

https://doi.org/10.5194/egusphere-2025-6216
Preprint. Discussion started: 20 January 2026

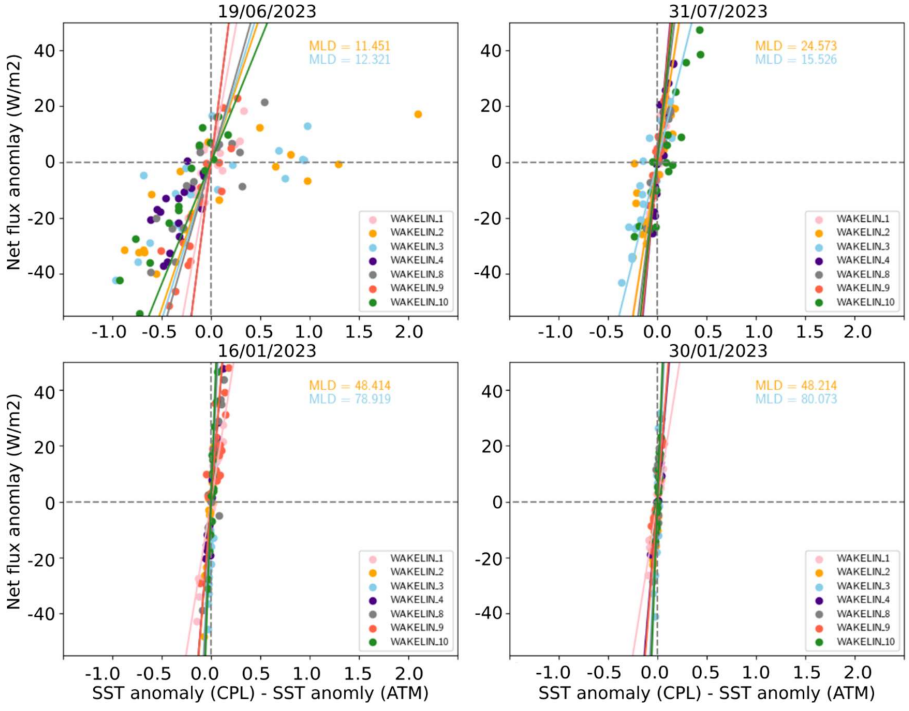

Figure 19: Net heat flux anomaly in coupled simulations averaged over hydrodynamically consistent regions (Wakelin *et al.*, 2012) **versus SST anomaly difference between coupled and atmosphere-only simulations for each ensemble member. Each panel shows a different case. SST anomaly is averaged over the last day, whereas net heat flux anomaly is averaged over the 5-day period. Solid lines indicate the average SST change computed using a simple mixed layer heat budget for each region.**

5 Unlocking new high frequency sea surface height disturbance forecasts (meteotsunamis)

In this final question, we explore a new area of forecasting opened up by 10mn coupling between km-scale models. A tsunami is a series of waves caused by the displacement of water. The displacement may result from 'bottom-up' seabed movement, such as that caused by earthquakes, landslides and volcanic eruptions or 'top-down' movement, from pressure perturbations in the atmosphere. These 'top-down' events are termed meteotsunamis. Their period is between 2 and 120 min: they are therefore resolved by the ocean model rather than the wave model. They are generated by mesoscale atmospheric perturbations traveling offshore, such as squalls, gravitational waves, hurricanes and weather fronts. These changes are usually only of a few hPa over a few tens of minutes which corresponds to a few centimetres of sea level change, via a process known as the inverse

https://doi.org/10.5194/egusphere-2025-6216
Preprint. Discussion started: 20 January 2026

barometric effect (Lewis *et al.*, 2023). As the waves triggered by the perturbations travel towards the shore, they can be amplified by multi-resonant mechanisms that can drive their amplitude up to a meter. Such mechanics include 1. Proudman resonance, where the propagation speed of the air disturbance matches that of the wave $\sqrt{gh}$, where g is the gravitational acceleration and h is the water depth, 2. self-amplification, where a meteotsunami traveling towards the shore increases in amplitude due to the decrease in water depth, 3. basin or harbour resonance, where the meteotsunami frequency is close to the resonant frequency of the basin or harbour that is traveling through 4. Greenspan response, where the speed of pressure perturbation traveling along the coast is close to the resonant speed along-shore edges (Renzi *et al.*, 2023).

In northwest Europe, meteotsunamis are less intense and frequent than in the US or the Adriatic Sea. Nevertheless, recent studies for the UK and Northwest Europe have shown that these events can cause significant disturbances and even be a high risk for coastal infrastructures, property and human life (Thompson *et al.*, 2020; Williams *et al.*, 2021; Lewis *et al.*, 2023; Renzi *et al.*, 2023). (Lewis *et al.*, 2023) produced a catalogue of events and showed their average frequency in the UK is around five per year, with one damaging event every five years. Currently, no early warning system is in place for this phenomenon in Northwest Europe.

The UK Environmental Agency reported coastal floods on 31/10/21 in the English Channel from Weymouth east to Portsmouth particularly Christchurch and Lymington. Impacts included flooding of quays, missed or late closure of tidal gates at Christchurch and Lymington. The Met Office surge forecast, forced with hourly global fields, did not indicate a surge near high tide, and no flood warning was issued. In this section, we investigate whether the km-scale coupled system with 10mn coupling frequency is able to represent and forecast this event, given its ability to explicitly resolve vertical motion in the atmosphere, its fine-scale bathymetry and coastline in a 1.5km ocean, and the possibility to exchange these fine-scale pressure perturbations every 10mn. UKC4 with 1h coupling (UKC4-1h) is compared with UKC4 with 10mn coupling (UKC4-10mn) to assess potential improvements in model performance. UKC4 here includes all changes described and evaluated in previous sections. Model outputs are validated against in situ observations from tide gauges to quantify accuracy.

5.1 Meteotsunami signal in sea surface height

To analyse the meteotsunami signal, we apply a high-pass Butterworth filter, a signal processing technique that attenuates low-frequency components while preserving high-frequency variations. Its calculation is:

$$H(s) = \frac{s^n}{s^n + \omega_c^n}$$

where $H(s)$ is the transfer function, s is the complex frequency variable, ω_c is the cutoff frequency, and n is the order of the filter. A 5th order high-pass Butterworth filter is used, with a 3h cutoff for filtering both sea surface height (SSH) and mean sea level pressure (MSLP). These filtering parameters effectively remove low-frequency background variations while preserving the key high-frequency components of meteotsunami-related atmospheric and oceanic disturbances.

Observations from the Portsmouth tide gauge (black line in Figure 20), where sea level is recorded every 15 minutes, indicate distinct positive anomalies on 31/10/21 at 07:00, 09:30, 15:00, more evident in the filtered time-series, where the peaks are

https://doi.org/10.5194/egusphere-2025-6216
Preprint. Discussion started: 20 January 2026

seen with a 2.5h frequency from 7:00 to 23:00. The 09:30 peak reached 24cm amplitude and was responsible for the coastal floods reported by the Environmental Agency. Simulations using the operational surge model (grey) and UKC4-1h (orange dashed line) largely reflect the lack of signal reported by the Environment Agency (EA). While both models forecast some anomalies (up to 9cm), they are too weak and occur around 12:00, after high tide. In contrast, UKC4-10mn (orange solid line) produces a 7cm change in sea level peaking at 08:45 during high tide, 15cm at 9:45, 30cm at 11:45, and further 10cm oscillations until 23:00, with a 2h frequency initially, which lengthens to 2.5h in the afternoon.

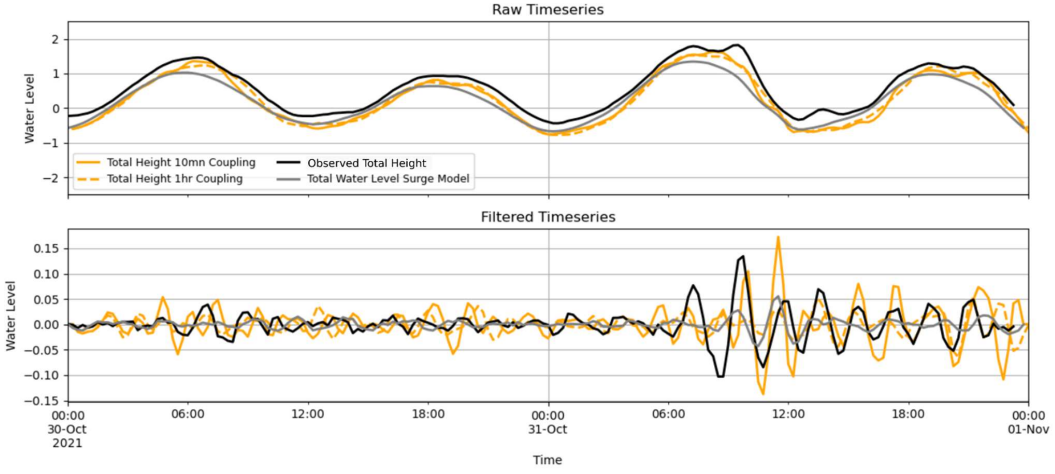

Figure 20: Raw output (top) and Butterworth high-pass filtered (bottom) sea surface height for UKC4-10mn (orange solid line), UKC4-1h (orange dashed line), and observations (black line) at Portsmouth tide gauge (cross in Fig. 21).

5.2 Atmospheric forcing

At the time of the event, a frontal system was moving across Ireland and the UK, ahead of a low pressure system centred on Ireland at 06:00 on 31/10/21 (Fig. 21a). It was associated with a band of heavy rainfall (>8mm/h) along the front (Fig. 21b). The dip in pressure is clearly seen in the 994 hPa isobar, on the coast of northern Brittany: a 50km-wide pressure disturbance and of 1-1.5hPa amplitude. It elongates from south-southwest to north-northeast across the English Channel (circled on figure). Convective activity within fronts is often responsible for strong, localised vertical wind speeds, and therefore, pressure disturbances of a few hPa.

https://doi.org/10.5194/egusphere-2025-6216
Preprint. Discussion started: 20 January 2026

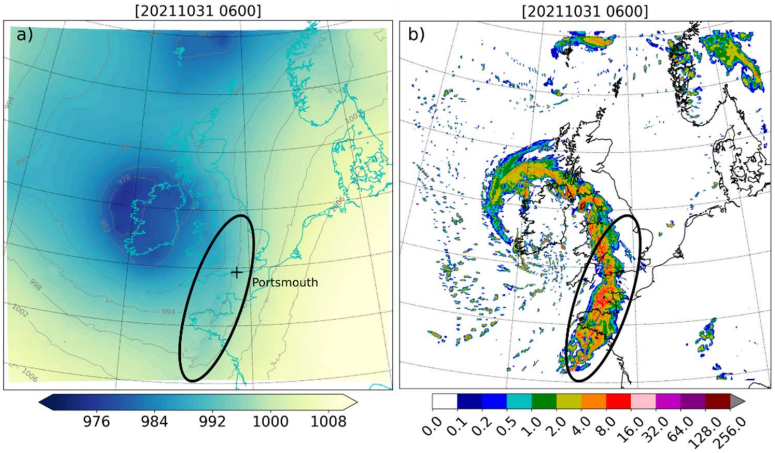

Figure 21: Atmospheric conditions on 31/10/2021 at 06:00UTC: a) mean sea level pressure (hPa) and b) hourly precipitation rate (mm/h).

Sea surface pressure timeseries spaced 100km apart across the English Channel (marked by stars in Fig. 22a) are shown in Fig. 22b. The frontal system is seen as a pressure drop at 02:00UTC on the western part of the Channel (blue), arriving at 08:30 just south of Portsmouth (red). This sudden pressure drop only lasts for 1h: 1-1.5hPa decrease for 30mn followed by 1-1.5hPa increase for 30mn. UKC4-1h (dashed lines) clearly misses this pressure drop, as 1h sampling frequency is too low to capture this short-lived pressure signal. This pressure disturbance associated with the front propagates with an estimated speed of 80 km/h. This closely matches the calculated phase speed of oceanic long waves in the English Channel, which is 60-90 km/h (Fig. 22a). The alignment of these speeds strongly suggests that the event was driven by Proudman resonance. Given the ocean model has 1.5km resolution, this means that every 10mn, the pressure disturbance is re-applied 9 grid points further along. The front takes 6h to travel from the blue to red point: the 1hPa disturbance, generating 1cm wave, is applied 36 times to the ocean, which is close to 30cm generated by the model.

https://doi.org/10.5194/egusphere-2025-6216
Preprint. Discussion started: 20 January 2026

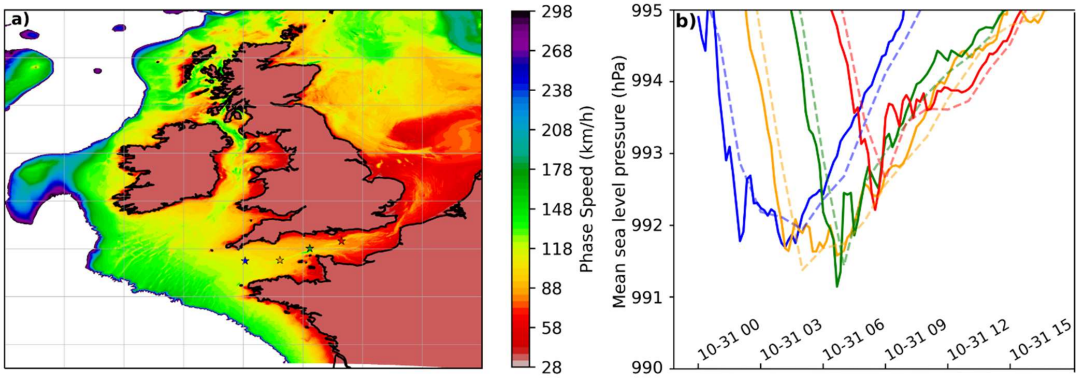

Figure 22: a) Phase speed calculated as $\sqrt{gh}$, with g being acceleration of gravity and h the local bathymetry; b) Timeseries of mean sea level pressure for the locations shown with stars on the phase speed map (a).

The spatial representation of the signal is shown in Figure 23. A low/high sea surface height (SSH) dipole emerges at the entrance of the Channel at 04:00. It propagates east, mostly visible along the UK coastline, at 06:00 and 09:00 the high SSH is near Portsmouth. It continues to propagate east at 10:15. At 12:00, the pressure disturbance is located in the southern North Sea, but the SSH signal is still visible, now with a positive signal in Northern France, negative signal in the middle of the Channel and positive signal in Portsmouth. This behaviour suggests the presence of seiching between the English and French coastlines, where oscillations become trapped within the Channel, where it is double the width of the perturbation (~100km), preventing immediate dispersion. Timeseries in two points confirm that the signal is anti-phased between the two coastlines (not shown). This explains that the anomaly persists in the afternoon of the 31/10/21, after the frontal system has moved away.

https://doi.org/10.5194/egusphere-2025-6216
Preprint. Discussion started: 20 January 2026

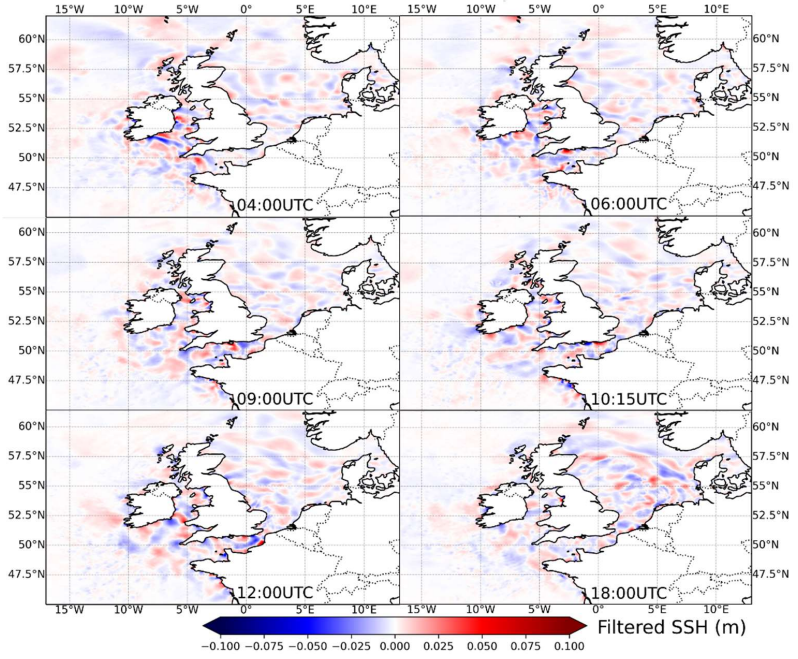

Figure 23: Spatial Sea Surface Height Filtered for times before the event on 30/10/2021 during the event (04:00-12:00), and during its dissipation (18:00).

5.3 Forecasting a meteotsunami with the UKC4 ensemble forecast

To assess the model's ability to forecast meteotsunami events, we performed ensemble simulations with lead times of one and three days. The filtered SSH for the 1-day forecast simulations is shown in Figure 24. In the one-day forecast, roughly six ensemble members successfully captured the meteotsunami throughout its full duration, predicting a signal of approximately 0.3 m. The ensemble shows the likelihood of an anomaly around the time of high tide (when the observed signal is maximal), which would have been useful information for the Environmental Agency. This reflects a relatively high level of accuracy at short lead times. In the three-day forecast (not shown), three ensemble members were still able to clearly reproduce the event, demonstrating the model's potential to deliver useful early warnings even several days ahead.

https://doi.org/10.5194/egusphere-2025-6216
Preprint. Discussion started: 20 January 2026

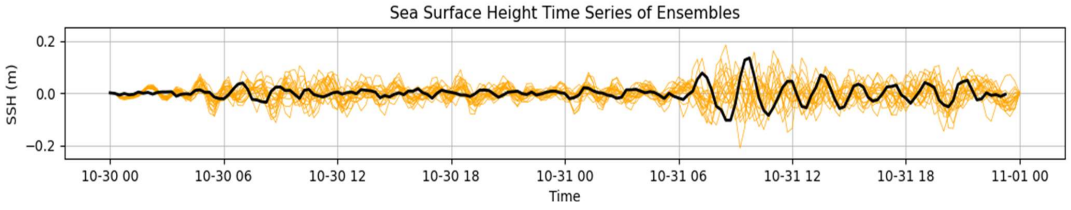

Figure 24: Meteotsunami ensemble forecast of filtered sea surface height (m) for Portsmouth location started 24h before the event. Each orange line is an ensemble member, and the black line is the observations.

8 Conclusions & perspectives

We presented an updated version of the Regional Coupled System – UK Coupled domain version four (RCS-UKC4), where substantial updates to component models have been made. Capability to run climate and near-real time ensemble capabilities have been introduced in addition to the previously supported deterministic case-study or longer hindcast modes. The river routing component has been substantially developed and improved. A new marine biogeochemistry component has also been added, as discussed in depth by (Partridge *et al.*, 2025). We have documented the development journey from individual model code and configuration updates to a final coupled configuration. This journey is made of compromises, as a one solution-fits-all is difficult to attain in coupled modelling. RCS-UKC4 includes a number of changes to coupling science choices, including to ocean light penetration parameters, coupling exchanges between atmosphere and waves, coupling frequency (with impact on ocean model timestep). Attempts to tune the wave growth parameter indicated keeping the UKC3 value balances optimal performance across wind, waves and SST. Importantly, developments to the Regional Coupled System workflow which is used to configure and run UKC4 simulations enables a flexible way of coupling various components of the system, and diversified the modes of running the UKC4 system: from ensemble weather forecasts, demonstrated here by running weekly in near-real time mode during winter and summer 2023, to multi-annual climate simulations, of which 4 years are analysed in this paper.

Changing the regional atmosphere model configuration in UKC4 had a large impact on heat budget reaching the ocean, and in particular the radiative terms. RAL3.3 has sufficient quality of surface fluxes over the ocean that multi-year simulations with the UKC4 system maintain domain-average seasonal SST bias of within 0.25°C, locally up to 1.5°C. Importantly, the SST does not drift from one year to another, indicating a balanced coupled system. Development of RCS-UKC4 has included assessment and enhancement to the representation of rivers in regional Met Office configurations, with reasonable geographic and temporal representation of broad-scale characteristics. Nevertheless, day-to-day streamflow variability tends to be underestimated in the west and north of the UK, and overestimated in the UK southeast. (Weedon *et al.*, 2023) recommend a change to saturated hydraulic conductivity in the soils to take into account bedrock properties, which will be a topic of research for the next coupled version.

https://doi.org/10.5194/egusphere-2025-6216
Preprint. Discussion started: 20 January 2026

In ensemble forecasting mode, UKC4 shows improved skill for ensemble wind and wave forecasting around the UK relative to its uncoupled model components, with better performance during storm events and in shallow regions where tidal energy dissipates through strong tidal currents. Nevertheless, it tends to underestimate extreme wind and waves and overestimate weak waves, although this is a common bias among models. This suggests that further improvements to the representation of boundary layer momentum mixing in high wind regimes is necessary for the next version of the regional coupled model. The effects of coupling on winds are reduced in UKC4 compared to UKC3, as the drag parameterisation in the new atmosphere and land configuration RAL3.3 is now closer to the WAVEWATCH III ST4 parameterisation. Compared to atmosphere-only simulations, coupling to a wave model reduces moderate wind speed and increases extratropical storm wind speeds, it also produces a larger variety of drag coefficients for a given wind speed, increasing spread around the drag/wind relationship. We also showed that a coupled system will tend to decrease the ensemble spread through negative SST/turbulent flux feedbacks, except in cases with a shallow mixed layer, where any changes in radiative fluxes between members (due to large-scale differences or perturbed parameters) can introduce large spread in the coupled system, independently from the SST perturbations imposed on the atmosphere.

Finally, coupled regional ensemble forecasts together with 10mn coupling frequency offer promises for early-warning system for meteotsunami hazards. We demonstrated that UKC4 is able to represent and forecast a relatively simple case of meteotsunami, which caused flooding on the southern coast of the UK. This event was very poorly captured in the current operational surge model. Makrygianni et al., (2025) explore a more complex meteotsunami case, also showing forecasting skills and fully explaining its complex atmospheric origin.

In summary, RCS-UKC4 has evolved to be a mature coupled modelling framework, suitable as a basis to provide future enhanced operational weather prediction capabilities. The Met Office has now integrated coupled experiments early in the development cycle of its Regional Atmosphere and Land configurations, which adds a constraint of good quality of RAL at the ocean surface (Bush *et al.*, 2024) and good quality of the land for river flow. The regional coupled system has also been demonstrated to be used to generate plausible climate simulations, and to help process-understanding complex compound phenomena such as marine heatwaves and their regional feedback on the atmosphere and land (Berthou et al., 2024), including during hazardous multi-hazard coastal events (Goswami *et al.*, 2025). Momentum partners across the world, and in particular over India, will benefit from these developments, and the sensitivity tests carried in this study will also be carried out over tropical domains (Thompson *et al.*, 2021; Castillo *et al.*, 2022).

Future research will assess the quality of UKC4 for multi-hazard forecasts and projections, will quantify the impacts of a km-scale regional coupled on regional climate change signal and will help quantify the current and future meteotsunami risks. The integration of biogeochemistry has already furthered our understanding of compound physical and biogeochemical events, such as waves, marine heatwaves and phytoplankton bloom interactions (Partridge *et al.*, 2025). Developments of wind farm parameterisations in the system will also enable to inform climate change mitigation strategies by helping the planning of

https://doi.org/10.5194/egusphere-2025-6216
Preprint. Discussion started: 20 January 2026

offshore wind farm development. Finally, long simulations with a high quality regional coupled system will enable to train machine learning models across multi-components of the earth system.

Code availability

Due to intellectual property right restrictions, neither the source code nor documentation papers for the Met Office Unified Model or JULES can be provided directly through open-source repositories. All model codes used within the RCS-UKC4 configuration are, however, accessible to registered researchers, and links to the relevant code licences and registration pages are provided for each modelling system below. Model code was provided to editor and reviewers at review time.

Obtaining the Unified Model. The Met Office Unified Model (UM) is available for use under a closed licence agreement. A number of research organizations and national meteorological services use the UM in collaboration with the Met Office to undertake research, produce forecasts, develop the UM code, and build and evaluate models. For further information on how to apply for a licence, please contact scientific_partnerships@metoffice.gov.uk. See also http://www.metoffice.gov.uk/research/modelling-systems/unified-model (last access: 5 January 2026). UM documentation papers are accessible to registered users at https://code.metoffice.gov.uk/doc/um/latest/umdp.html (last access: 5 January 2026).

Obtaining JULES. The Joint UK Land Environment Simulator (JULES) is freely available to any researcher for non-commercial use. Further information on requesting access and the JULES terms and conditions are accessible via http://jules-lsm.github.io/access_req/JULES_access.html (Clark et al., 2011). The JULES user manual is available at https://jules-lsm.github.io/ (last access: 5 January 2026).

Obtaining the flexible configuration management system. The UM and JULES codes were built using the fcm_make extract and build system provided within the flexible configuration management (FCM) tools. UM and JULES codes and Rose suites were also configuration-managed using this system. FCM releases can be obtained via a GitHub repository at https://doi.org/10.5281/zenodo.4775250 (Shin et al., 2021) and https://github.com/metomi/fcm/releases (last access: 5 January 2026), under a GNU General Public License. Further information and user documentation are provided at http://metomi.github.io/fcm/doc/user_guide/ (last access: 5 January 2026).

Obtaining Rose and Cylc. The Rose framework was used for defining UM–JULES workflows. This is free software available under a GNU General Public License. Further details are available at https://doi.org/10.5281/zenodo.15169210 (Shin et al., 2025) and https://github.com/metomi/rose (last access: 5 January 2026). Cylc is a general-purpose workflow engine that

https://doi.org/10.5194/egusphere-2025-6216
Preprint. Discussion started: 20 January 2026

manages and runs cycling systems, including UM–JULES workflows. It is available under a GNU General Public License. Further details are available at https://cylc.github.io (last access: 5 January 2026) and Oliver et al. (2019).

Obtaining RAL3 workflows and configuration Workflows used in development of RCS-UKC4 are available to any licensed user of both the UM and JULES via the Met Office Science Repository Service (MOSRS) via https://code.metoffice.gov.uk/trac/roses-u (last access: 5 January 2026). Further support for using MOSRS is provided at https://code.metoffice.gov.uk/trac/home (last access: 5 January 2026).

Obtaining NEMO The model code for NEMO vn4.0.4 is available from the NEMO website (https://www.nemo-ocean.eu/, last access: 7 January 2026). After registration the Fortran code is readily available to researchers.

Obtaining WAVEWATCH III The WAVEWATCH III® code base is distributed by NOAA National Weather Service Environmental Modeling Center under an open-source-style licence via https://polar.ncep.noaa.gov/waves/wavewatch/wavewatch.shtml (last access: 7 January 2026). Interested readers wishing to access the code are requested to register to obtain a licence via https://polar.ncep.noaa.gov/waves/wavewatch/license.shtml (last access: 5 January 2026). The model is subject to continuous development, with new releases generally becoming available to those interested and committed to basic model development, subject to agreement. Model codes used in the RCS-IND1 system are maintained under configuration management via a mirror repository hosted at the Met Office.

Obtaining OASIS3-MCT OASIS3-MCT vn2.0 is disseminated to registered users as free software from https://oasis.cerfacs.fr/en/ (last access: 5 January 2026; OASIS3-MCT development team, 2026).

Data availability

Code and data used in the production of figures in this paper are available via https://doi.org/10.5281/zenodo.17957427 (Berthou et al. (2025b)).

Author contributions

SB prepared the manuscript with contributions from all co-authors. JMC, CS, AA, NM, SM, VFL, HL all contributed to develop the regional coupled modelling infrastructure, run the experiments and analyse results. The other authors contributed by either providing help in developing the system, its forcing data or by reviewing the manuscript.

https://doi.org/10.5194/egusphere-2025-6216
Preprint. Discussion started: 20 January 2026

Competing interests

No competing interests.

Disclaimer

Copernicus Publications remains neutral with regard to jurisdictional claims made in the text, published maps, institutional affiliations, or any other geographical representation in this paper. While Copernicus Publications makes every effort to include appropriate place names, the final responsibility lies with the authors. Views expressed in the text are those of the authors and do not necessarily reflect the views of the publisher.

Acknowledgements

Thank you to Lewis Blunn, James Warner, Richard W. Jones for their help to run near-real time cases in summer 2023. The development and assessment of the Regional Coupled UK domain version 4 configuration is possible only through the contributions of a large number of people, which exceeds the list of authors of this paper. We would particularly wish to acknowledge the underpinning development and maintenance of the technical tools that support this endeavour, notably all code developers of the Unified Model, JULES, NEMO, WaveWatchIII and ERSEM, and those who support use of tools and workflows to run simulation experiments and analyse their outputs.

Financial support

This work and its contributors were funding by the Met Office Hadley Centre Climate Programme funded by DSIT and by the Met Office Weather and Climate Science for Service Partnership (WCSSP) India project which is supported by the UK Department for Science, Innovation & Technology (DSIT). WCSSP India is a collaborative initiative between the Met Office and the Indian Ministry of Earth Sciences (MoES).

Review statement

The review statement will be added by Copernicus Publications listing the handling editor as well as all contributing referees according to their status anonymous or identified.

https://doi.org/10.5194/egusphere-2025-6216
Preprint. Discussion started: 20 January 2026

References

Ardhuin F., Rogers E., Babanin A V., Filipot JF., Magne R., Roland A., van der Westhuysen A., Queffeulou P., Lefevre JM., Aouf L., Collard F. 2010. Semiempirical Dissipation Source Functions for Ocean Waves. Part I: Definition, Calibration, and Validation. *J Phys Oceanogr* 40:1917–1941.

Barrett P., Abel S., Lean H., Price J., Stein T., Stirling A., Darlington T. 2021. WesCon 2023: Wessex UK Summertime Convection Field Campaign. *EGU21*.

Berthou S., Renshaw R., Smyth T., Tinker J., Grist JP., Wihsgott JU., Jones S., Inall M., Nolan G., Berx B., Arnold A., Blunn LP., Castillo JM., Cotterill D., Daly E., Dow G., Gómez B., Fraser-Leonhardt V., Hirschi JJ-M., Lewis HW., Mahmood S., Worsfold M. 2024. Exceptional atmospheric conditions in June 2023 generated a northwest European marine heatwave which contributed to breaking land temperature records. *Commun Earth Environ* 5:287.

Berthou S., Siddorn J., Fraser-Leonhardt V., Le Traon P-Y., Hoteit I. 2025a. Towards Earth system modelling: coupled ocean forecasting. *State of the Planet* 5-opsr:20.

Berthou, S. (2025b). RCS-UKC4 configuration paper data and code [Data set]. Zenodo. https://doi.org/10.5281/zenodo.17957427

Best MJ., Beljaars A., Polcher J., Viterbo P. 2004. A Proposed Structure for Coupling Tiled Surfaces with the Planetary Boundary Layer. *J Hydrometeorol* 5:1271–1278.

Best MJ., Pryor M., Clark DB., Rooney GG., Essery R. LH., Ménard CB., Edwards JM., Hendry MA., Porson A., Gedney N., Mercado LM., Sitch S., Blyth E., Boucher O., Cox PM., Grimmond CSB., Harding RJ. 2011. The Joint UK Land Environment Simulator (JULES), model description – Part 1: Energy and water fluxes. *Geosci Model Dev* 4:677–699.

Bidlot JR. 2020. Enhancing tropical cyclone forecasts. *ECMWF Newsletter*.

Brooks RJ., Corey AT. 1964. Hydraulic properties of porous media.

Brown AR., Milton S., Cullen M., Golding B., Mitchell J., Shelly A. 2012. Unified modelling and prediction of weather and climate: a 25 year journey. *Bull. Am. Meteorol. Soc.* 93:1865–1877.

Bruciaferri D., Tonani M., Lewis HW., Siddorn JR., Saulter A., Castillo Sanchez JM., Valiente NG., Conley D., Sykes P., Ascione I., McConnell N. 2021. The Impact of Ocean-Wave Coupling on the Upper Ocean Circulation During Storm Events. *J Geophys Res Oceans* 126:e2021JC017343.

Bruggeman J., Bolding K. 2014. A general framework for aquatic biogeochemical models. *Environmental Modelling & Software* 61:249–265.

Bush M., Allen T., Bain C., Boutle I., Edwards J., Finnenkoetter A., Franklin C., Hanley K., Lean H., Lock A., Manners J., Mittermaier M., Morcrette C., North R., Petch J., Short C., Vosper S., Walters D., Webster S., Weeks M.,

https://doi.org/10.5194/egusphere-2025-6216
Preprint. Discussion started: 20 January 2026

Wilkinson J., Wood N., Zerroukat M. 2020. The first Met Office Unified Model–JULES Regional Atmosphere and Land configuration, RAL1. *Geosci Model Dev* 13:1999–2029.

Bush M., Boutle I., Edwards J., Finnenkoetter A., Franklin C., Hanley K., Jayakumar A., Lewis H., Lock A., Mittermaier M., Mohandas S., North R., Porson A., Roux B., Webster S., Weeks M. 2023. The second Met Office Unified Model–JULES Regional Atmosphere and Land configuration, RAL2. *Geosci Model Dev* 16:1713–1734.

Bush M., Flack DLA., Lewis HW., Bohnenstengel SI., Short CJ., Franklin C., Lock AP., Best M., Field P., McCabe A., Van Weverberg K., Berthou S., Boutle I., Brooke JK., Cole S., Cooper S., Dow G., Edwards J., Finnenkoetter A., Furtado K., Halladay K., Hanley K., Hendry MA., Hill A., Jayakumar A., Jones RW., Lean H., Lee JCK., Malcolm A., Mittermaier M., Mohandas S., Moore S., Morcrette C., North R., Porson A., Rennie S., Roberts N., Roux B., Sanchez C., Su C-H., Tucker S., Vosper S., Walters D., Warner J., Webster S., Weeks M., Wilkinson J., Whitall M., Williams KD., Zhang H. 2024. The third Met Office Unified Model-JULES Regional Atmosphere and Land Configuration, RAL3. *Geoscientific Model Development Discussions* 2024:1–58.

Butenschön M., Clark J., Aldridge JN., Icarus Allen J., Artioli Y., Blackford J., Bruggeman J., Cazenave P., Ciavatta S., Kay S., Lessin G., Van Leeuwen S., Van Der Molen J., De Mora L., Polimene L., Sailley S., Stephens N., Torres R. 2016. ERSEM 15.06: A generic model for marine biogeochemistry and the ecosystem dynamics of the lower trophic levels. *Geosci Model Dev* 9:1293–1339.

Castillo JM., Lewis HW., Mishra A., Mitra A., Polton J., Brereton A., Saulter A., Arnold A., Berthou S., Clark D., Crook J., Das A., Edwards J., Feng X., Gupta A., Joseph S., Klingaman N., Momin I., Pequignet C., Sanchez C., Saxby J., da Costa M. 2022. The Regional Coupled Suite (RCS-IND1): application of a flexible regional coupled modelling framework to the Indian region at kilometre scale. *Geosci Model Dev* 15:4193–4223.

Cavaleri L., Abdalla S., Benetazzo A., Bertotti L., Bidlot J-R., Breivik Ø., Carniel S., Jensen RE., Portilla-Yandun J., Rogers WE., Roland A., Sanchez-Arcilla A., Smith JM., Staneva J., Toledo Y., van Vledder GPh., van der Westhuysen AJ. 2018. Wave modelling in coastal and inner seas. *Prog Oceanogr* 167:164–233.

Cullen MJP. 1993. The unified forecast/climate model. *Meteorol. Mag.* 122:81–94.

Durnford D., Fortin V., Smith GC., Archambault B., Deacu D., Dupont F., Dyck S., Martinez Y., Klyszejko E., MacKay M., Liu L., Pellerin P., Pietroniro A., Roy F., Vu V., Winter B., Yu W., Spence C., Bruxer J., Dickhout J. 2018. Toward an Operational Water Cycle Prediction System for the Great Lakes and St. Lawrence River. *Bull Am Meteorol Soc* 99:521–546.

Fallmann J., Lewis H., Sanchez JC., Lock A. 2019. Impact of high-resolution ocean–atmosphere coupling on fog formation over the North Sea. *Quarterly Journal of the Royal Meteorological Society* 145:1180–1201.

Field PR., Hill A., Shipway B., Furtado K., Wilkinson J., Miltenberger A., Gordon H., Grosvenor DP., Stevens R., Van Weverberg K. 2023. Implementation of a double moment cloud microphysics scheme in the UK met office regional numerical weather prediction model. *Quarterly Journal of the Royal Meteorological Society* 149:703–739.

https://doi.org/10.5194/egusphere-2025-6216
Preprint. Discussion started: 20 January 2026

Fortin V., Abaza M., Anctil F., Turcotte R. 2014. Why Should Ensemble Spread Match the RMSE of the Ensemble Mean? *J Hydrometeorol* 15:1708–1713.

Gedney N., Cox PM. 2003. The sensitivity of global climate model simulations to the representation of soil moisture heterogeneity. *J. Hydrometeorol.* 4:1265–1275.

Gentile ES., Gray SL., Barlow JF., Lewis HW., Edwards JM. 2021. The Impact of Atmosphere–Ocean–Wave Coupling on the Near-Surface Wind Speed in Forecasts of Extratropical Cyclones. *Boundary Layer Meteorol* 180:105–129.

Gentile ES., Gray SL., Lewis HW. 2022. The sensitivity of probabilistic convective-scale forecasts of an extratropical cyclone to atmosphere–ocean–wave coupling. *Quarterly Journal of the Royal Meteorological Society* 148:685–710.

van Genuchten MT., Leji FJ., Yates SR. 1991. *The RETC code for quantifying the hydraulic functions of unsaturated soils.*

Good S., Fiedler E., Mao C., Martin MJ., Maycock A., Reid R., Roberts-Jones J., Searle T., Waters J., While J., Worsfold M. 2020. The Current Configuration of the OSTIA System for Operational Production of Foundation Sea Surface Temperature and Ice Concentration Analyses. *Remote Sens (Basel)* 12.

Goswami P., Berthou S., Shepherd TG., Volonté A., Mahmood S., Castillo JM., Péquignet A-C., Park Y-J., Worsfold M., Rodrigues R., Balmaseda MA. 2025. Marine heatwave amplifies extreme multi-hazards of extratropical cyclone Babet. *EGUsphere* 2025:1–26.

Graham JA., O'Dea E., Holt J., Polton J., Hewitt HT., Furner R., Guihou K., Brereton A., Arnold A., Wakelin S., Castillo Sanchez JM., Mayorga Adame CG. 2018. AMM15: a new high-resolution NEMO configuration for operational simulation of the European north-west shelf. *Geosci Model Dev* 11:681–696.

Guiavarc'h C., Roberts-Jones J., Harris C., Lea DJ., Ryan A., Ascione I. 2019. Assessment of ocean analysis and forecast from an atmosphere–ocean coupled data assimilation operational system. *Ocean Science* 15:1307–1326.

Hersbach H., Bell B., Berrisford P., Hirahara S., Horányi A., Muñoz-Sabater J., Nicolas J., Peubey C., Radu R., Schepers D., Simmons A., Soci C., Abdalla S., Abellan X., Balsamo G., Bechtold P., Biavati G., Bidlot J., Bonavita M., De Chiara G., Dahlgren P., Dee D., Diamantakis M., Dragani R., Flemming J., Forbes R., Fuentes M., Geer A., Haimberger L., Healy S., Hogan RJ., Hólm E., Janisková M., Keeley S., Laloyaux P., Lopez P., Lupu C., Radnoti G., de Rosnay P., Rozum I., Vamborg F., Villaume S., Thépaut J-N. 2020. The ERA5 global reanalysis. *Quarterly Journal of the Royal Meteorological Society* 146:1999–2049.

Holt J., Hyder P., Ashworth M., Harle J., Hewitt HT., Liu H., New AL., Pickles S., Porter A., Popova E., Allen JI., Siddorn J., Wood R. 2017. Prospects for improving the representation of coastal and shelf seas in global ocean models. *Geosci Model Dev* 10:499–523.

Janssen P. 1991. Quasi-linear theory of wind-wave generation applied to wave forecasting. *J Phys Oceanogr*.

Janssen P. 2004. *The interaction of ocean waves and wind*. Cambridge University Press.

https://doi.org/10.5194/egusphere-2025-6216
Preprint. Discussion started: 20 January 2026

Kendon EJ., Rowell DP., Jones RG. 2010. Mechanisms and reliability of future projected changes in daily precipitation. *Clim Dyn* 35:489–509.

Komaromi WA., Reinecke PA., Doyle JD., Moskaitis JR. 2021. The Naval Research Laboratory's Coupled Ocean–Atmosphere Mesoscale Prediction System-Tropical Cyclone Ensemble (COAMPS-TC Ensemble). *Weather Forecast* 36:499–517.

Lea DJ., While J., Martin MJ., Weaver A., Storto A., Chrust M. 2022. A new global ocean ensemble system at the Met Office: Assessing the impact of hybrid data assimilation and inflation settings. *Quarterly Journal of the Royal Meteorological Society* 148:1996–2030.

Lewis HW., Castillo Sanchez JM., Arnold A., Fallmann J., Saulter A., Graham J., Bush M., Siddorn J., Palmer T., Lock A., Edwards J., Bricheno L., la Torre A., Clark J. 2019a. The UKC3 regional coupled environmental prediction system. *Geosci Model Dev* 12:2357–2400.

Lewis HW., Dadson SJ. 2021. A regional coupled approach to water cycle prediction during winter 2013/14 in the United Kingdom. *Hydrol Process* 35:e14438.

Lewis HW., Manuel Castillo Sanchez J., Graham J., Saulter A., Bornemann J., Arnold A., Fallmann J., Harris C., Pearson D., Ramsdale S., Martínez-De La Torre A., Bricheno L., Blyth E., Bell VA., Davies H., Marthews TR., O'Neill C., Rumbold H., O'Dea E., Brereton A., Guihou K., Hines A., Butenschon M., Dadson SJ., Palmer T., Holt J., Reynard N., Best M., Edwards J., Siddorn J. 2018. The UKC2 regional coupled environmental prediction system. *Geosci Model Dev* 11:1–42.

Lewis H., Sanchez J., Siddorn J., King R., Tonani M., Saulter A., Sykes P., Pequignet C., Weedon G., Palmer T., Staneva J., Bricheno L. 2019b. Can wave coupling improve operational regional ocean forecasts for the North-West European Shelf? *Ocean Science* 15:669–690.

Lewis C., Smyth T., Williams D., Neumann J., Cloke H. 2023. Meteotsunami in the United Kingdom: the hidden hazard. *Natural Hazards and Earth System Sciences* 23:2531–2546.

Li JG. 2022. Hybrid multi-grid parallelisation of WAVEWATCH III model on spherical multiple-cell grids. *J Parallel Distrib Comput* 167:187–198.

MacLachlan C., Arribas A., Peterson D., Maidens A., Fereday D., Scaife AA., Gordon M., Vellinga M., Williams A., Comer RE., Camp J., Xavier P., Madec G. 2015. Global Seasonal forecast system version 5 (GloSea5): a high-resolution seasonal forecast system. *Q. J. R. Meteorol. Soc.* 141:1072–1084.

Madec G., Delacluse P., Imbard M., Levy C. 1998. *OPA Version 8.1 Ocean General Circulation Model Reference Manual*.

Mahmood S., Lewis H., Arnold A., Castillo J., Sanchez C., Harris C. 2021. The impact of time-varying sea surface temperature on UK regional atmosphere forecasts. *Meteorological Applications* 28:e1983.

https://doi.org/10.5194/egusphere-2025-6216
Preprint. Discussion started: 20 January 2026

Makrygianni N., Berthou S., Flack DLA., Lebeaupin Brossier C., Beuvier J., Castillo JM., Renzi E., O'Neill C., Peláez-Zapata D., Dias F., Lewis H., Bruciaferri D. 2025. Meteotsunami prediction in km-scale regional systems coupled at high frequency. *EGUsphere* 2025:1–41.

Moore RJ. 1985. The probability distributed principle and runoff production at point and basin scales. *Hydrolog. Sci. J.* 30:273–297.

OASIS3-MCT development team. OASIS3-MCT coupling libraries, OASIS [code], https://oasis.cerfacs.fr/en/ (last access: 5 January 2026), 2026.

Oliver, H., Shin, M., Matthews, D., Sanders, O., Bartholomew, S., Clark, A., Fitzpatrick, B., van Haren, R., Hut, R., and Drost, N.: Workflow Automation for Cycling Systems, Comput. Sci. Eng., 21, 7–21, https://doi.org/10.1109/MCSE.2019.2906593, 2019.

Partridge D., Berthou S., Millington R., Clark J., Bricheno L., Castillo JM., Rulent J., Lewis H. 2025. Impact of waves on phytoplankton activity on the Northwest European Shelf: insights from observations and km-scale coupled models. *EGUsphere* 2025:1–32.

Patmore R., O'Dea E., Bruciaferri D., Wakelin S., Harle J., Wise A., Byrne D., Polton J. 2023. JMMP-Group/CO_AMM15: CO9_p2.0.

Porson AN., Carr JM., Hagelin S., Darvell R., North R., Walters D., Mylne KR., Mittermaier MP., Willington S., Macpherson B. 2020. Recent upgrades to the Met Office convective-scale ensemble: An hourly time-lagged 5-day ensemble. *Quarterly Journal of the Royal Meteorological Society* 146:3245–3265.

Renault L., Marchesiello P. 2022. Ocean tides can drag the atmosphere and cause tidal winds over broad continental shelves. *Communications Earth & Environment 2022 3:1* 3:1–7.

Renzi E., Bergin C., Kokina T., Pelaez-Zapata DS., Giles D., Dias F. 2023. Meteotsunamis and other anomalous "tidal surge" events in Western Europe in Summer 2022. *Physics of Fluids* 35:46605.

Ruti PM., Somot S., Giorgi F., Dubois C., Flaounas E., Obermann A., Dell'Aquila A., Pisacane G., Harzallah A., Lombardi E., Ahrens B., Akhtar N., Alias A., Arsouze T., Aznar R., Bastin S., Bartholy J., B??ranger K., Beuvier J., Bouffies-Cloch?? S., Brauch J., Cabos W., Calmanti S., Calvet JC., Carillo A., Conte D., Coppola E., Djurdjevic V., Drobinski P., Elizalde-Arellano A., Gaertner M., Gal??n P., Gallardo C., Gualdi S., Goncalves M., Jorba O., Jord?? G., L'Heveder B., Lebeaupin-Brossier C., Li L., Liguori G., Lionello P., Maci??s D., Nabat P., ??nol B., Raikovic B., Ramage K., Sevault F., Sannino G., Struglia M V., Sanna A., Torma C., Vervatis V. 2016. Med-CORDEX initiative for Mediterranean climate studies. *Bull Am Meteorol Soc* 97:1187–1208.

Sheldon L., Czaja A., Vannière B., Morcrette C., Sohet B., Casado M., Smith D. 2017. A 'warm path' for Gulf Stream–troposphere interactions. *Tellus A: Dynamic Meteorology and Oceanography* 69:1299397.

Shin, M., Fitzpatrick, B., Matthews, D., Pillinger, T., Whitehouse, S., Cresswell, P., Clark, A., Oxley, S., Dix, M., Sharp, R., and Mancell, J.: metomi/fcm: (2021.05.0), Zenodo [code], https://doi.org/10.5281/zenodo.4775250, 2021. a

https://doi.org/10.5194/egusphere-2025-6216
Preprint. Discussion started: 20 January 2026

Shin, M., Fitzpatrick, B., Clark, A., Sanders, O., Pillinger, T., Dutta, R., Bartholomew, S. L., Whitehouse, S., Matthews, D., Oxley, S., Trzeciak, T., Valters, D., Oliver, H. J., Mancell, J., Hall, M., Coleman, T., Shepherd, H., Osprey, A., Seddon, J., Theodorakis, D., Joe, R., Abram, J., Dix, M., Sharp, R., metofcm, Frost, J., Dawson, M., and Cresswell, P.: metomi/rose: Rose 2.4.2 (2.4.2), Zenodo [code], https://doi.org/10.5281/zenodo.15169210, 2025.

Smith RNB. 1990. A scheme for predicting layer clouds and their water content in a general circulation model. *Q. J. R. Meteorol. Soc.* 116:435–460.

Somot S., Ruti P., Ahrens B., Coppola E., Jordà G., Sannino G., Solmon F. 2018. Editorial for the Med-CORDEX special issue. *Clim Dyn* 51:771–777.

Tennant W., Beare S. 2014. New schemes to perturb sea-surface temperature and soil moisture content in MOGREPS. *Quarterly Journal of the Royal Meteorological Society* 140:1150–1160.

Thompson J., Renzi E., Sibley A., Tappin DR. 2020. UK meteotsunamis: a revision and update on events and their frequency. *Weather* 75:281–287.

Thompson B., Sanchez C., Heng BCP., Kumar R., Liu J., Huang X-Y., Tkalich P. 2021. Development of a MetUM (v 11.1) and NEMO (v 3.6) coupled operational forecast model for the Maritime Continent – Part 1: Evaluation of ocean forecasts. *Geosci Model Dev* 14:1081–1100.

Tolman HL., the WWIII development group. 2014. User Manual and System Documentation of WAVEWATCH III® Version 4.18.

Tonani M., Pequignet C., King R., Sykes P., McConnell N., Siddorn JR. 2019. *Copernicus Marine Environment Monitoring Service Quality Information Document North West European Shelf Production Centre NORTHWESTSHELF_ANALYSIS_FORECAST_PHYS_004_013*. Exeter.

Valcke S. 2013. The OASIS3 coupler: a European climate modelling community software. *Geosci. Model Devel.* 6:373–388.

Valiente NG., Saulter A., Edwards JM., Lewis HW., Castillo Sanchez JM., Bruciaferri D., Bunney C., Siddorn J. 2021. The Impact of Wave Model Source Terms and Coupling Strategies to Rapidly Developing Waves across the North-West European Shelf during Extreme Events. *J Mar Sci Eng* 9.

Valiente NG., Saulter A., Gomez B., Bunney C., Li JG., Palmer T., Pequignet C. 2023. The Met Office operational wave forecasting system: the evolution of the regional and global models. *Geosci Model Dev* 16:2515–2538.

Vannière B., Czaja A., Dacre H., Woollings T. 2017. A "Cold Path" for the Gulf Stream–Troposphere Connection. *J Clim* 30:1363–1379.

Wahle K., Staneva J., Koch W., Fenoglio-Marc L., Ho-Hagemann HTM., Stanev E V. 2017. An atmosphere–wave regional coupled model: improving predictions of wave heights and surface winds in the southern North Sea. *Ocean Science* 13:289–301.

Wakelin SL., Holt JT., Blackford JC., Allen JI., Butenschön M., Artioli Y. 2012. Modeling the carbon fluxes of the northwest European continental shelf: Validation and budgets. *J Geophys Res Oceans* 117.

https://doi.org/10.5194/egusphere-2025-6216
Preprint. Discussion started: 20 January 2026

Weedon GP., Robinson EL., Bloomfield JP., Turner S., Crane EJ., Best MJ. 2023. Geological controls of discharge variability in the Thames Basin, UK from cross-spectral analyses: Observations versus modelling. *J Hydrol (Amst)* 625:130104.

Weverberg K Van., Morcrette CJ., Boutle I., Furtado K., Field PR. 2021. A Bimodal Diagnostic Cloud Fraction Parameterization. Part I: Motivating Analysis and Scheme Description. *Mon Weather Rev* 149:841–857.

Williams DA., Schultz DM., Horsburgh KJ., Hughes CW. 2021. An 8-yr Meteotsunami Climatology across Northwest Europe: 2010–17. *J Phys Oceanogr* 51:1145–1161.

Wilson DR., Ballard SP. 1999. A microphysically based precipitation scheme for the UK Meteorological Office Unified Model. *Q. J. R. Meteorol. Soc.* 125:1607–1636.